



MINING MACHINES

2022

volume 40, Issue 3

Quarterly of Science and Technology

e-ISSN 2719-3306



MINING MACHINES

2022, Vol. 40 Issue 3

CONTENTS:

Pages 121-122

Author: Małgorzata MALEC

Prof. Adam Klich – in memoriam

Pages 123-129

Authors: Tomasz KORBIEL, Stefan CZERWIŃSKI

Keeping mining machinery in operation based on energy factors

Pages 130-140

Authors: Stanisław SZWEDA, Marek WOJTASZCZYK, Tibor KRENICKY

Tests of selected elements of building components in the light of compulsory requirements

Pages 141-148

Authors: Tamer RIZAOĞLU, Canberk ÇOŞKUN, Murat CAMUZCUOĞLU

Determination of physical and mechanical properties of limestones used as marble in Tut-Adiyaman Region in Turkey

Pages 149-157

Author: Henryk BADURA

Analysis of one-day forecasts of the maximum methane concentration in a tailgate of a longwall ventilated with U system - a case study

Pages 158-172

Author: Łukasz BOŁOZ

Use of the iLogic Autodesk Inventor tool in the process of designing self-propelled drilling rigs

Pages 173-179

Authors: Paweł KAMIŃSKI, Darian BOŽIČ

Shaft reaming machine for maintenance of mine shafts in the salt rock mass



e-ISSN 2719-3306

Quarterly of Science and Technology

October 2022

Editorial Staff

Editor – in – Chief

Dariusz Prostański, KOMAG Institute of Mining Technology, POLAND

Managing Editor

Marzena Pabian-Macina, KOMAG of Mining Technology, POLAND

Thematic Editors

Scientific discipline

Environment engineering, mining and power engineering

Greg Galecki, Missouri University of Science and Technology, UNITED STATES

Carsten Drebenstedt, Technische Universität Bergakademie Freiberg, GERMANY

Automation, electronics and electrotechnics

Joel M. Haight, University of Pittsburgh, Pittsburgh, UNITED STATES

Krzysztof Fajarewicz, Silesian University of Technology, POLAND

Mechanical engineering

Brian D. Ricketts, European Association for Coal and Lignite (EURACOAL), BELGIUM

Jarosław Brodny, Silesian University of Technology, POLAND

Pavol Bozek, Slovak University of Technology in Bratislava, SLOVAK REPUBLIC

English Language Editor

Dominik Brandys, University of Washington in Seattle, UNITED STATES

Statistical Editor

Jarosław Tokarczyk, KOMAG Institute of Mining Technology, POLAND

Open Access Leader

Adrianna Kalita, KOMAG of Mining Technology, POLAND

Publishers and contact

KOMAG Institute of Mining Technology

Pszczyńska 37, 44-101 Gliwice, POLAND

E-mail of Editorial Office: miningmachines@komag.eu

Editor-in-Chief

phone: +48 32 2374600

e-mail: dprostanski@komag.eu

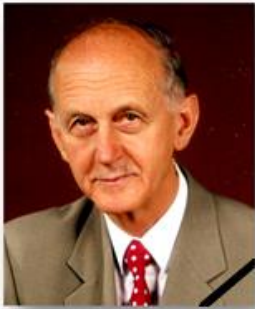
Managing Editor

phone: +48 32 2374612

e-mail: mmacina@komag.eu

<http://komag.eu/publications/mining-machines/editorial-office>

PROF. ADAM KLICH – IN MEMORIAM



With a great regret and grief the Management, Scientific Council and Employees of the KOMAG Institute of Mining Technology received the information that Prof. Adam Klich passed away on 12th August 2022. He was the Member of the KOMAG Scientific Council over the years 1973-2015 and its Chairman for three terms of office over the years 1988-1999.

For many years he was Scientific Editor of the KOMAG monographs and publications as well as a reviewer of scientific articles and conference papers.

Prof. Klich was a dedicated scientist and researcher, specializing in issues of occupational safety and ergonomics in the mining industry. He was very active in the field of scientific development of the KOMAG young staff of researchers, whom he supported on their difficult path of getting scientific degrees. The results of his work have a measurable dimension as within the period of fifteen years forty KOMAG researchers gained Ph. D. degrees in technical science.

Prof. Klich's achievements at KOMAG include activities oriented onto a high scientific standard of publications, presenting results of scientific, development and technical projects conducted by the KOMAG researchers, in particular examples of industrial implementations of innovative solutions of mining machines and equipment.

Prof. Klich took part in scientific-and-technical conferences, organized by KOMAG, sharing his interdisciplinary knowledge and scientific experience with representatives of academia and industry.

As the Scientific Editor of monographs: KOMEKO, KOMTECH, CYLINDER and SHAFT TRANSPORT he paid special attention to scientific honesty, reliability and genuineness.

The subject-matter of Prof. Klich's scientific activity covered innovative cutting of minerals, safe systems of shaft transport in mines, new designs of machines and equipment for roadway workings.

Prof. Klich and his co-workers from the AGH University of Science and Technology initiated several scientific projects whose results contributed to a development of the mining industry in Poland and abroad.

His collaboration with many foreign scientific institutions in the Slovak Republic, in the Czech Republic, in Hungary, in Germany, in Ukraine, in Russia and in Romania should be highlighted. The results of his research and development projects were presented at various conferences abroad, where he started collaborative links with American, Canadian, Japanese, Chinese, British, French and Indian scientists.

Prof. Klich's output of publications consists of more than 300 articles in Polish and foreign scientific magazines, 4 books, 2 monographs and 4 student's books. He owned 55 patent – letters.

In recognition of outstanding scientific achievements and their implementation into industrial practice, and also for a rich and creative collaboration with scientific institutions in Poland and



abroad, the Senate of the AGH University of Science and Technology rewarded Prof. Adam Klich with the Title of Honorary Professor.

Prof. Klich will be remembered for ever not only as an outstanding scientist who was always ready to help all those who needed his assistance and scientific support, but mainly as a very good, noble-minded person, who was full of optimism and faith that even most difficult problems could be solved due to tolerance and strong will to reach a compromise. For His co-workers He was always a model of modesty and ability of discovering in people their best and most valuable features of character.

Grateful for a multi-year, fruitful collaboration and all the activities oriented onto a scientific development of the KOMAG Institute, Prof. Klich's co-workers from KOMAG will always remember Him.

Requiescat in Pace!



Małgorzata Malec
KOMAG Institute of Mining Technology

<https://doi.org/10.32056/KOMAG2022.3.1>

Keeping mining machinery in operation based on energy factors

Received: 12.07.2022

Accepted: 15.09.2022

Published online: 11.10.2022

Author's affiliations and addresses:

¹ AGH University of Science and Technology, Faculty of Mechanical Engineering and Robotics, Department of Mechanics and Vibroacoustics, al. Mickiewicza 30, 30-059 Krakow, Poland

² *retiree*

* Correspondence:

e-mail: tkorbiel@agh.edu.pl

Tomasz KORBIEL  ^{1*}, **Stefan CZERWIŃSKI** ²

Abstract:

Mining machinery maintenance strategy based on the current dynamic condition of the equipment not only improves reliability, reduces repair and renovation costs, but also affects electricity costs. Due to the use of modern monitoring and diagnostic systems, as well as advanced control and supervision methods, it is possible to improve the efficiency of devices and thus reduce energy costs. Due to the high power of the devices, even a slight decrease in efficiency translates into significant financial resources. Taking into account the prices of electricity as well as ecological aspects, investments in modern solutions give specific financial and social savings.

Keywords: maintenance, technical diagnostics, energy indicator



1. Introduction

One of the main costs in the mining plant includes the costs of electric energy. In relation to the mine specificity they constitute 20-48% of all the costs which shape the production efficiency directly [1]. The main expenses cover dewatering, ventilation and run-of-mine haulage as well as its preparation systems. In the case of ventilation devices, their unit powers vary in the section from 750 kW to 1.5 MW. A few (2-3) fan stations and air treatment stations are operated in the central ventilation system. Pumps of the power 1-2 MW are used for the mine central dewatering system and their number depends on an inflow of underground water. The haulage process incorporates armoured face conveyors equipped with 3 drives of the power 300 kW, a beam stage loader of the power about 200 kW, the sectional haulage system consisting of a few (3-5) conveyors with a double drive of 200 kW and the main haulage system composed of a few (2-5) belt conveyors with multiple (2-4) drives of the power in order of 200 kW. The presented specification is of exemplary character. The parameters depend on the type of operation, the distance of the longwall under mining and the specificity of a given mining plant. Only main receivers of electric energy, which will be used for indicating guidelines of operational maintenance based on energy indicators, are mentioned.

Each electric machine transforms electric energy into a different kind of energy, including mechanical, potential energy with a certain, finite efficiency. The devices, mentioned above, are complex and the energy is transformed in them in a few stages. For example, the energy factor of dewatering will indicate electric energy consumption needed for pumping a determined amount of water from the assumed depth within the assumed time. As the depth of the main dewatering operations can be regarded as the constant, so for a given case this factor will be expressed in kWh/m³ [2]. Electric energy is transformed into torque of the pump shaft at a given angular velocity, then onto energy of hydrostatic pressure. This pressure causes a flow of water in the collector which rises the water mass to a given height and velocity of its outflow at the collector outlet. Similarly, a complex transformation takes place in other devices [3]. In the case of the haulage system, at a given longwall, the energy factor will be expressed in kWh/t of transported run-of-mine [4]. Obviously, the value of this factor will depend on the distance of the working from the transport shaft, however in the case of a given location, together with a geometry of the haulage route, this factor will be connected with efficiency of individual components of the haulage system.

Relative values of presented energy factors, to a large extent, depend on efficiency coefficients of individual components transforming energy. The efficiency of these components depends, among others, on their technical condition. Therefore, a maintenance of machines in a good technical conditions has a direct impact on the costs of electric energy. Although this thesis seems to be common, it is not always noticed. A general analysis of a few selected systems in an exemplary mining plant will be conducted to illustrate these costs. Taking into consideration a contemporary geopolitical situation, increasing costs of electric energy as well as prospects of power transformation, the presented analysis can be useful in the scope of taking strategic decisions connected with maintaining operations.

2. Materials and Methods

Exploitational costs of a longwall shearer-equipped system

In complex systems of energy transformation, the total efficiency is a product of partial efficiencies. Therefore, an efficiency improvement of any component has a direct impact on the total efficiency and thus on the energy efficiency. Taking into consideration exemplary devices in the longwall shearer-equipped system (Fig. 1), the following energy consuming devices can be indicated, together with their power (Table 1) and main energy transforming systems.



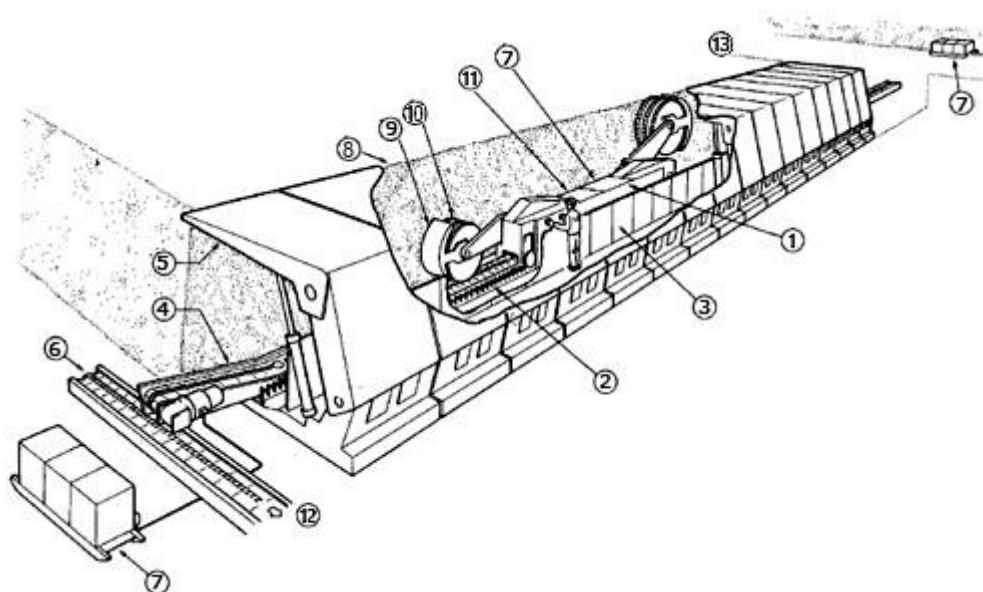


Fig. 1. Devices in the longwall shearer-equipped system:

- 1 – Shearer, 2 – Toothed Bar, 3 – Spill-plate, 4 – Armoured Face Conveyor, 5 – Longwall Support, 6 – Beam Stage Loader, 7 – Electric Apparati Box, 8 – Longwall Face, 9 – Loader, 10 – Cutting Drum, 11 – Haulage Unit, 12 – Tail-end Gate, 13 – Head-Gate

Table 1. Exemplary power of devices in the longwall system

Drive of Shearer	1.0 MW
Hydraulic Supply of Supports	0.1 MW
Armoured Face Conveyor	0.8 MW
Beam Stage Loader	0.2 MW
Crusher	0.1 MW

From the specification, given above, it can be concluded that the power consumption of the longwall system, subject to an analysis, reaches 2.2 MW. In in-situ conditions the current consumption varies from 1.5 MW to 2.5 MW, in the case of complex and difficult seams. The given electric power, is transformed in electric motors into torque. Efficiencies of contemporary electric drives of medium power exceed 94% and for big powers - even 97%. It is a reaction to the European Union Directive EuP 2005/32/EC and to the Regulation of the European Commission 640/2009 ordering an application of energy – saving motors. The rated efficiency can be different from the exploitaltional efficiency. Different factors such as: a number of start-ups, cooling systems, dynamics of mechanical loading etc. [5] have an impact on the exploitaltional efficiency. For example incorrect parameters of motor cooling can reduce its efficiency by even 6%. The efficiency decreases when the operational period decreases and each general overhaul can reduce the efficiency by 4%. The condition of bearings, the condition of winding, the rectilinearity of the shaft line also have an impact on the motor efficiency. A poor technical condition of these components reduces the efficiency even by 10%.

3. Analysis of exploitaltional costs - Results

An exemplary longwall system of the rated power 2.2 MW showed the energy consumption on the level of 1 GWh during the monthly accounting period. This value depends on many external factors, so it cannot be the condition estimator. However, based on this information some savings, resulting from the exploitaltional policy, can be achieved. For example, an incorrect operation of the cooling system of the longwall shearer motor, which causes an increase of the motor temperature below the warning thresholds, can cause an efficiency drop on the level of 2% [6-7]. Assuming a proportional

electric energy consumption by a shearer, its monthly consumption will reach 0.45 GWh. An efficiency drop by 2% causes an increase of consumption on the level of 9 MWh during the monthly period. This cost would be connected only with an incorrect servicing of the cooling system. Similar calculations can be performed for other mechanical components and in the case when several irregularities occur, an increase of energy consumption in the range of several dozen MWh will be experienced.

As it is not possible to show irregularities in drive systems based on energy factors, other methods based on monitoring and diagnostics of mechanical systems [8-12] should be applied. A detection and a repair of even small irregularities at the first sight will give serious savings in the scope of electric energy consumption [13].

In the case of the central dewatering systems, the cost of electric energy dominates. Basic components of the dewatering costs have been estimated on the example of the main dewatering pump having typical parameters as given below:

- capacity $Q = 500 \text{ m}^3/\text{h}$,
- height of rise $H = 800 \text{ m}$.

Dewatering costs are composed of:

- investment costs;
- costs of electric energy for the pump drive. The pump of given parameters consumes the power in the order of 1.5 MW. A typical main dewatering pump is operated about 10 hours per day, i.e. 300 hours monthly. It gives the monthly energy consumption in the range of 450 MWh.
- costs of repairs;
- costs of servicing.

From the assessment, presented above, the following conclusions can be drawn:

- The cost of energy, generating over 90% of total costs, dominates in the total cost of dewatering operations with use of a typical main dewatering pump. Therefore, a reduction of dewatering costs should concentrate on a reduction of energy consumption.
- The cost of consumed energy depends on energy efficiency of pumps to a large extent. In difficult mine conditions the initial efficiency of the pump assembly, delivered by the producer, is subject to a change and in a longer period the cost of consumed energy depends on the overhaul policy, which has a decisive impact on an average efficiency of pumps during their operation.

For the parameters, given above, the efficiency of the pump assembly should be at least on the level of 75%, for which the power consumption will reach 1453 kW. However, if the assembly efficiency of such parameters reached 70%, then the power consumption would increase to 1557 kW and for the efficiency of 65% - to 1676 kW. As it can be seen, in the case of above given parameters such a reduction of efficiency means an increase of power consumption in the range of 200 kW. If a pump operates for 10 hours daily, i.e. 300 hours monthly, it gives an increase of power consumption in the order of 60 MWh.

From the point of view of energy efficiency, the amount of energy consumed for pumping 1 m^3 is essential. There is a certain unit value of energy, which should be consumed for pumping the liquid to the height H_g . A minimal value of the e_1 indicator – a consumption of power pumping 1 m^3 of liquid, expressed in kWh/m^3 , is its measure [14]. Minimal value of this indicator – $e_{1,\min}$, assuming an ideal flow of liquid is determined by the formula:

$$e_{1,\min} = N_{\min}/Q = 3,6 \cdot 10^{-3} \cdot \gamma \cdot H_g$$

where:

- N_{\min} – minimal power of pump assembly, kW,
- Q – capacity of pump assembly, m^3/h ,
- γ – liquid specific gravity, kN/m^3 ,
- H_g – geometric height to which the water is pumped, m.



This factor enables to assess the energy efficiency of a given dewatering system by comparing the real energy consumption for pumping one cubic meter with the minimal consumption. Getting below this minimal unit energy consumption is impossible physically. However, during an exploitation it should be attempted that the real unit energy consumption is higher than the minimum to the possible smallest degree. As it can be concluded from the analyses presented above, the energy demand depends on:

- real efficiency of the pump assembly η_z , which is smaller than one. The overhaul policy and a selection of the pump for the system have the biggest impact on the value of energy efficiency of the pump assembly,
- values of losses in pipelines,
- exploitative policy.

In the case of the main dewatering system, the loading of the system is stationary and therefore the unit energy indicator is a measure of the system efficiency [2]. The following factors have a significant impact on the energy efficiency:

- technical condition of the motor,
- condition of the motor and pumps bearings,
- axiality of shafts lines, condition of clutch,
- rigidity of machine foundation,
- sludge content in water gates,
- collaboration of pumps operated on one collector,
- condition of filters and flaps,
- condition of pipelines.

Each of the mentioned factors has an impact on general efficiency and each 1% of the efficiency drop causes additional monthly costs in the range of 4.5 MWh as in the presented example.

Fan stations are equipped with fans of the power in the range of 750 kW÷1.1 MW. Mining plants possess 2-3 upcast shafts, so the total power of the ventilation system is 2÷3 MW. Fan stations are operated in a continuous mode, so it is possible to indicate a monthly energy consumption of electric energy on the level 1.5÷2.2 GWh. This calculation does not take into an account the systems for air treatment as well as methane drainage systems. An output of the ventilation system depends on the arrangement of underground gates, used local ventilation systems and additional flow resistance occurring in the mine. Due to this reason, the energy factor cannot be used for an assessment of fans technical conditions, however this condition has a direct impact on energy demand. Environmental factors, affecting the output of ventilation system, are regarded to be slow-changing and therefore sudden changes of the energy indicator can signal an incorrect operation of fan station.

Fan stations give a possibility of controlling exploitative parameters which depend on environmental conditions. Due to that it is possible to optimize costs by appropriate control algorithms [15, 16]. In this case savings can even reach 5% of the energy demand.

Another factor, enabling to improve the energy factor, includes diagnostic systems [17, 18]. Due to an early detection of failures the system reliability is increased, which is the priority in this case. It is possible to prevent against destructive processes which have an impact on energy factor. Calculating an average power of a fan station on the level of 1 MW, the monthly demand of electric energy is 720 MWh. Therefore, each 1% of efficiency causes about 7 MWh of additional energy costs.

4. Conclusions

Efficiency of high power machines, operated in a continuous mode, directly and significantly influences electric energy consumption and therefore the costs of exploitation. In relation to the machine class, the policy of its exploitation, loading and control, a series of methods enabling, in an indirect or direct way, to monitor efficiency parameters, can be indicated. In these cases even a minor irregularities can cause essential costs. Therefore, an immediate maintenance personnel's reaction can contribute to an improvement of the economic balance. The most important methods include:



- specialistic diagnostic and monitoring systems of technical condition,
- advanced control systems, optimized from the point of view of reducing energy consumption,
- exact compliance with the requirements specified in the technical manual, with particular attention paid to overhauls, check-ups and maintenance activities,
- care about exploitation materials, lubricants,
- high competences of servicing personnel.

The presented recommendations and methods are more and more significant in the context of increasing costs of electric energy as well as climatic policy.

References

- [1] Ochab B., Kaliś H.: Optymalizacja kosztów energii elektrycznej w Zakładach Górniczo-Hutniczych 'Bolesław' S.A. w Bukownie. *Przegląd Górniczy*, 2005, vol. 61, no. 1
- [2] Korbiel T., Wojciechowski J.: Analiza kosztów eksploatacji systemu głównego odwadniania kopalni węgla kamiennego. *Syst. Wspomagania w Inżynierii Prod.*, 2019, vol. 8, no. 11, pp. 413–419
- [3] Mocek P., Smoliło J.: Optymalizacji parametrów sieci wentylacyjnej kopalni X w przypadku likwidacji jednego z szybów wentylacyjnych. *Systemy Wspomagania w Inżynierii Produkcji*, 2019, vol. 8, no. 1, pp. 203–221
- [4] Czerwiński S.: Ocena efektów ekonomicznych kompleksów ścianowych. *Zeszyty Naukowe. Organizacja i Zarządzanie, Politechnika Śląska*, 2011, vol. 59, pp. 219–233
- [5] Pontt J.: High-power drives for energy efficiency and abatement of carbon emissions in mineral processing, *Proc. IEEE Int. Conf. Ind. Technol.*, 2010, pp. 5–10
- [6] Krok R.: Badanie wpływu temperatury otoczenia na sprawność silnika indukcyjnego. *Maszyny Elektryczne, Zesz. Probl.*, 2018, vol. 2, no. 118, pp. 19–22
- [7] Figura R., Szychta L., Szychta E.: Wyznaczanie współczynnika sprawności silnika klatkowego pracującego ze zmienną prędkością obrotową. *Zesz. Probl., Masz. Elektr.*, 2011, vol. 90, pp. 163–168
- [8] Barszcz T., Randall R. B.: Application of spectral kurtosis for detection of a tooth crack in the planetary gear of a wind turbine, *Mechanical Systems and Signal Processing*, 2009, vol. 23, issue 4, pp. 1352-1365, doi: 10.1016/j.ymssp.2008.07.019
- [9] Barszcz T., Jabłoński A.: A novel method for the optimal band selection for vibration signal demodulation and comparison with the Kurtogram. *Mechanical systems and signal processing*, 2011, vol. 25, issue 1, pp. 431-451, doi: 10.1016/j.ymssp.2010.05.018
- [10] Zimroz R., Bartelmus W., Barszcz T., Urbanek J.: Diagnostics of bearings in presence of strong operating conditions non-stationarity—A procedure of load-dependent features processing with application to wind turbine bearings. *Mechanical systems and signal processing*, 2014, vol. 46, issue 1, pp. 16-27 doi: 10.1016/j.ymssp.2013.09.010
- [11] Dybała J., Zimroz R.: Empirical Mode Decomposition of Vibration Signal for Detection of Local Disturbances in Planetary Gearbox Used in Heavy Machinery System, *Key Eng. Mater.*, 2014, vol. 588, pp. 109–116
- [12] Wyłomańska A., Obuchowski J., Zimroz R., Hurd H.: Periodic Autoregressive Modeling of Vibration Time Series From Planetary Gearbox Used in Bucket Wheel Excavator. *Cyclostationarity: Theory and methods*. Springer, Cham, 2014, pp. 171–186, doi: 10.1007/978-3-319-04187-2_12
- [13] Korbiel T., Biały W., Czerwiński S.: Ocena stanu technicznego maszyn górniczych w oparciu o kryterium rozkładu Weibulla. *Syst. Wspomagania w Inżynierii Prod.*, 2016, vol. z. 1 (13)
- [14] Jędral W.: Efektywność energetyczna pomp i instalacji pompowych. *Krajowa Agencja Poszanowania Energii S.A. Warszawa 2007. ISBN 978-83-921049-3-3*
- [15] Babu V. R., Maity T., Burman S.: Optimization of energy use for mine ventilation fan with variable speed drive. *2016 Int. Conf. on Intell. Control. Power and Instrumentation (ICICPI)*, 2016, pp. 148–151
- [16] Schutte A. J., Kleingeld M., Van Der Zee L.: An integrated energy efficiency strategy for deep mine ventilation and refrigeration. *2014 International Conference on the Eleventh industrial and Commercial Use*



of Energy. IEEE, 2014. p. 1-9.

- [17] Bian L., Sun H., He H., Liu C., Guan Z.: Research on fault diagnosis of mine ventilator bearing based on cross entropy algorithm. 2020 35th Youth Acad. Annu. Conf. Chinese Assoc. of Autom. (YAC). IEEE, 2020, pp. 407–411
- [18] Farjow W., Daoud M., Fernando X. N.: Advanced diagnostic system with ventilation on demand for underground mines. 34th IEEE Sarnoff Symp., 2011, pp.1-6



<https://doi.org/10.32056/KOMAG2022.3.2>

Tests of selected elements of building components in the light of compulsory requirements

Received: 27.07.2022

Accepted: 02.09.2022

Published online: 11.10.2022

Author's affiliations and addresses:

¹ KOMAG Institute of Mining
Technology, Pszczyńska 37,
44-101 Gliwice, Poland

² Faculty of Manufacturing
Technologies of the Technical
University of Košice with a seat in
Prešov, Bayerova 1, 080-01 Prešov,
Slovak Republic

* Correspondence:

e-mail: sszweda@komag.eu

Stanisław SZWEDA ^{1*}, Marek WOJTASZCZYK ¹,
Tibor KRENICKY ²

Abstract:

A procedure of standard strength tests of reinforcement bars conducted at present at the ITG KOMAG is discussed. Taking advantage of the bibliographic review, concerning tests of reinforced concrete with steel reinforcement bars, a possibility of using the KOMAG testing infrastructure to broaden the scope of tests of reinforcement bars was analyzed. Due to a more and more common use of composite bars for reinforcing and strengthening concrete structures, the methods of testing their strength properties are discussed. The conditions enabling to conduct strength tests of composite reinforced concrete bars at the ITG KOMAG are determined.

Keywords: steel reinforcement bars, strength tests, composite reinforcement bars, pullout test of bars, bar adhesion test to concrete



1. Introduction

The KOMAG Laboratory of Tests, apart from a broad scope of tests of mining machines and equipment, also conducts tests for other branches of economy. Among others, based on the agreement concluded with Regional Building Supervision Inspectorates, the Laboratory realizes strength tests of reinforcement bars. A necessity of conducting such tests results from the Act [1]. Simultaneously, a development of materials used for reinforcing concrete elements, causing a need of conducting tests of cognitive character, can be noticed. New grades of steel for reinforcing concrete are used which generates a necessity of experimental check-up of requirements as regards their suitability. Impact tests of some physical features of reinforcement bars on the parameters of reinforced structure forces e.g.: a need of testing the strength of reinforced beams [2] are indispensable. Composite reinforcement bars are implemented more and more frequently. An identification of mechanical properties of such bars is connected with a need of conducting laboratory tests not only of the composite but also of the reinforced concrete element, where a composite bar is used.

This publication is oriented onto an analysis of possibilities of performing strength tests concerning both reinforcement bars made of steel and composite as well as complete reinforced concrete elements with such bars.

2. Materials and Methods

2.1. Procedure of strength testing of steel reinforcement bars realized at the ITG KOMAG

Tests of steel for reinforcing concrete are conducted on the basis of the agreement with Regional Building Supervision Inspectorates. According to [1] and [3] the procedure of tests includes:

- the information about the producer of the building product under testing,
- the identification data of the element under testing,
 - a) the designation of the series or production lot,
 - b) the size of production lot, from which a sample is taken,
 - c) the data concerning date of sampling and manner of its packaging.

The data, mentioned above, in a form of the minutes, are forwarded to the Laboratory together with the samples, which are to be subject to tests, in a form of reinforcement bars of the length 0.5 m, taken at the construction site.

In the Laboratory, after having conducted a visual inspection and having confirmed that their number and condition enable to conduct the ordered tests, the tensile test of all the delivered samples is conducted to determine the following parameters:

- sample strength in the yield point – R_e ,
- sample tensile strength – R_m ,
- ratio of stresses:

$$k = \frac{R_m}{R_e} \quad (1)$$

- total elongation at the maximum force – A_{gt} .

An exemplary set of measurement results of the parameters, mentioned above, is given in Table 1. Using the obtained measurement results, it is possible to check if the marked strength parameters of samples meet the declared useful properties determined in the minutes of sampling the construction product.

In the case of samples whose test results are presented in Table 1, the declared properties of the construction product, subject to the tests of a given scope, are:

- sample strength in the yield point – $500 \text{ MPa} \leq R_e \leq 625 \text{ MPa}$
- ratio of stresses – $1.15 \leq k \leq 1.35$
- total elongation at the maximum force – $A_{gt} \geq 8 \%$.



In the case under consideration, it was stated that the tested samples met the declared properties of a construction product.

Table 1. Exemplary tests results of bar samples made of ribbed steel for reinforcing concrete [4]

No. of sample	Yield point	Tensile strength	Ratio of stresses	Total elongation at maximum force
	R_e [MPa]	R_m [MPa]	R_m/R_e	A_{gt} [%]
1	570 ± 2.9	675 ± 3.4	1.18	10.0 ± 0.1
2	578 ± 2.9	674 ± 3.4	1.17	10.4 ± 0.1
3	573 ± 2.9	673 ± 3.4	1.17	10.3 ± 0.1
4	575 ± 2.9	677 ± 3.4	1.18	10.2 ± 0.1
5	583 ± 2.9	675 ± 3.4	1.16	10.6 ± 0.1
6	580 ± 2.9	675 ± 3.4	1.16	10.1 ± 0.1
7	573 ± 2.9	679 ± 3.4	1.19	10.6 ± 0.1
8	581 ± 2.9	675 ± 3.4	1.16	10.9 ± 0.1
9	581 ± 2.9	675 ± 3.4	1.16	10.7 ± 0.1
10	585 ± 2.9	677 ± 3.4	1.16	10.5 ± 0.1

Since 2020 in total 41 sets of samples of steel reinforcement bars have been subject to tests. It should be highlighted that no samples, characterized by the strength properties differing from the values declared by the producer in the minutes of forwarding samples for tests, have been identified. The samples for tests have usually been taken from the steel lot for reinforcing concrete which has just been delivered to the construction site. In the conclusion it can be stated that positive results of performed tests confirm reliable work of producers of reinforcement bars.

2.2. Tests of steel reinforcement bars in the light of standards and research projects

The scope of tests of reinforcement bars, recommended by the Regional Building Supervision Inspectorates, does not encompass all the tests included in the standards [5] and [6], for example the tests of the bar adhesion to concrete. In appendices of the standard [5] two methods of testing an adhesion of bars – the beam method and the pullout method are described in detail. The described methods differ from each other significantly which causes that the results, obtained with their use, serve mainly for a qualitative comparison of adhesion of bars having a similar diameter but different shape of the surface [7].

A diagram of a rig for testing an adhesion with use of the beam method for testing bars of the diameter smaller than 16 mm (according to [5] – beam of A) type is presented in Fig 1.

The reinforcement bar under testing is fixed centrally in the bottom part of two concrete blocks 6, situated on supports 3 and connected with a steel articulated joint 4 in the top part. The articulated joint enables bending of the beam without transmitting an additional load to blocks 6. The reinforcement bar adheres to the concrete only on two sections of the total length of $20 \cdot d$ (where: d – bar diameter). The system of blocks under testing is subject to bending until a total loss of adhesion or a bar break occurs. A general view of the test rig is presented in Fig. 2. A way of fixing the displacement recorder of the bar end is shown in Fig. 3.



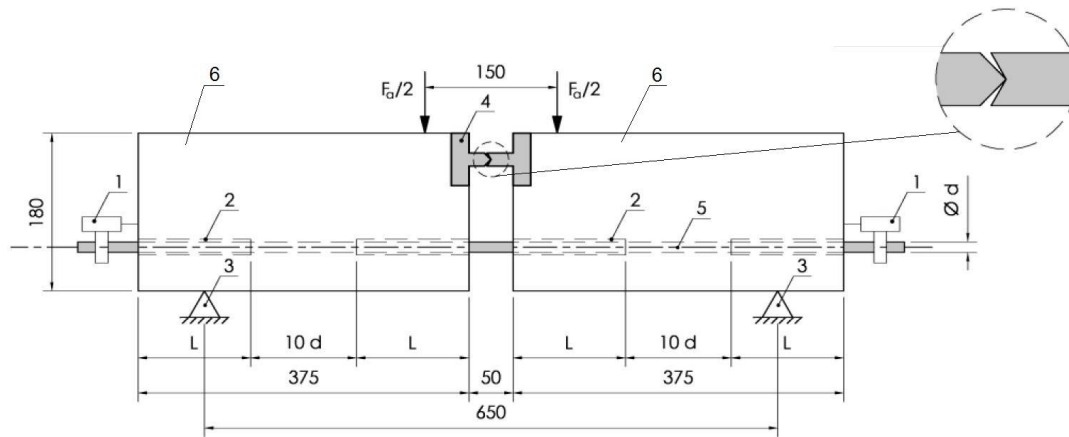


Fig. 1. Rig for testing an adhesion of a reinforcement bar with use of the beam method [7]
 1 – measurement system, 2 – plastic sleeve, 3 – support,
 4 – steel articulated joint, 5 – reinforcement bar under testing, 6 – concrete block
 F_a – force loading the beam, d – bar diameter, L – sleeve length



Fig. 2. View of a test rig [8]



Fig. 3. Fixation of the displacement recorder of the bar end [8]

During the test the graph: force – slip (of the bar) is recorded and an average stress of the adhesion at slip– τ_b [5] is determined:

$$\tau_b = \frac{\sigma_s}{40} \tag{2}$$

where:

σ_s – stress in the bar determined from the relationship:

$$\sigma_s = \frac{1.25 \cdot F_a}{A_n} \quad \text{for } d < 16 \text{ mm} \tag{3}$$

$$\sigma_s = \frac{1.50 \cdot F_a}{A_n} \quad \text{for } d \geq 16 \text{ mm} \tag{4}$$

F_a – force loading the beam (see Fig. 1) for a given value of slip,
 A_n – rated area of the bar cross-section.

Using the graph: force – slip and values of adhesion stresses at slip, an assessment of the bar adhesion is conducted. A preparation of the rig for a test is extremely time – consuming, and according to [5] the test should be performed for 25 samples of the bar.

The method of testing an adhesion of a reinforcement bar to concrete with use of pullout method is presented schematically in Fig. 4. The bar under testing is placed inside a concrete cube 1, touching the concrete only at the top section of the length equal to „5·d”. The cube 1 is situated on a steel support 6 with a hole, where a longer, bottom section of the bar is put through.

The test consists in loading the bar bottom end with tensile force, generated by the MTS machine 4, until the sample is damaged or the bar is broken. The force, tensioning the bar – F_a and a displacement of the bar top end – Δ_a are recorded. An adhesion of the bar to concrete is assessed based on the graph $F_a = f(\Delta_a)$ [5].

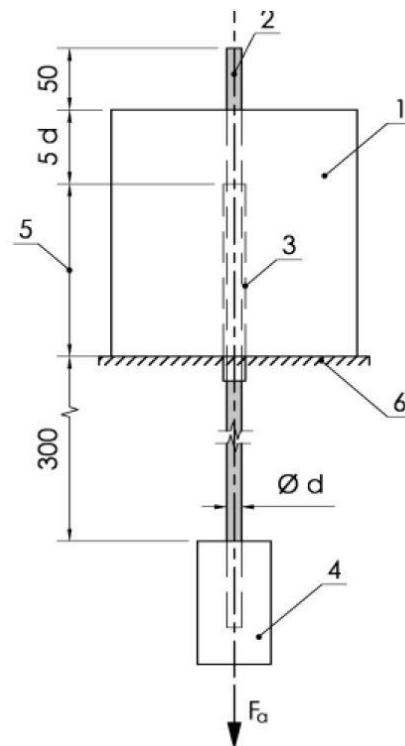


Fig. 4. Diagram of test of reinforcement adhesion using the pullout method [7]

1 – concrete cube, 2 – bar under testing, 3 – plastic sleeve, 4 – grip of the MTS machine,
5 – free length of bar, 6 – support with hole

The attempts of pulling out a reinforcement bar from a concrete block, described in the literature, differ as regards the method of preparing a sample and the conditions at the contact: concrete-steel platen [9]. A diagram of the test rig is shown in Fig. 5.

A soft rubber washer and a layer of plastic, decreasing friction, are placed between the block and the plate to minimize a disadvantageous impact between the concrete block and the rig as well as the differences in the state of stresses in the concrete and the steel platen [10]. A slip of the bar is measured directly with use of two displacement transducers (LVDT). Due to a modified setup of the rig a significant reduction of random fluctuations of measurement results is obtained.

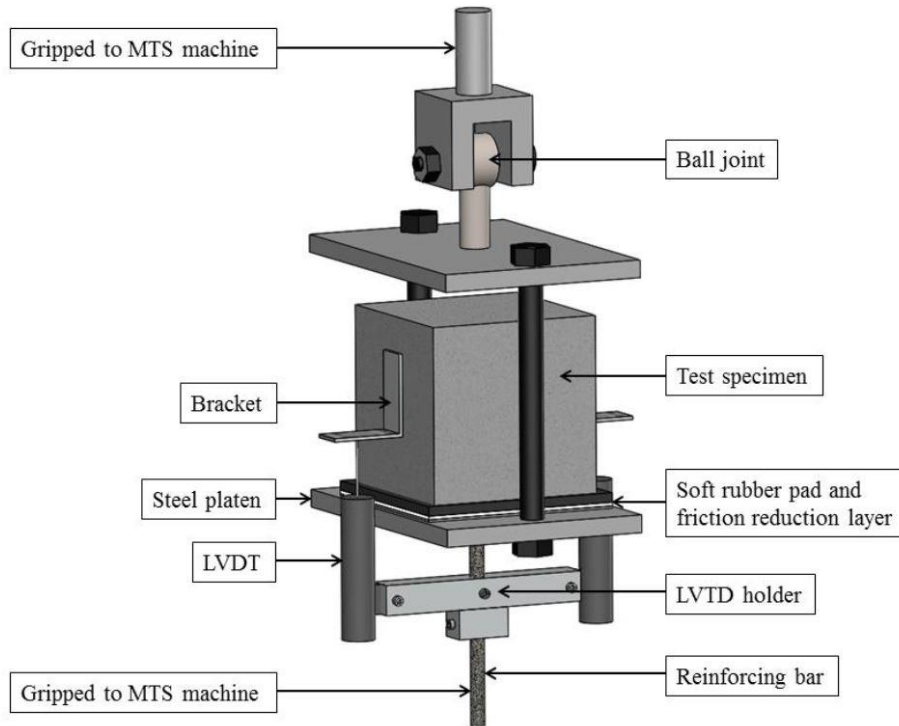


Fig. 5. Schematic diagram of pullout test setup [9]

Apart from adhesion tests of the reinforcement bar to the concrete, the mechanical properties of steel in relations to reinforcement and prestressing of concrete, according to [5] and [6], are also determined in the following tests: fatigue test, bend test, rebend test and fatigue test at axial loading. A diagram of the device used for a realization of transverse bend and rebend tests are shown in Fig. 6 and a course of the rebend test is shown in Fig. 7.

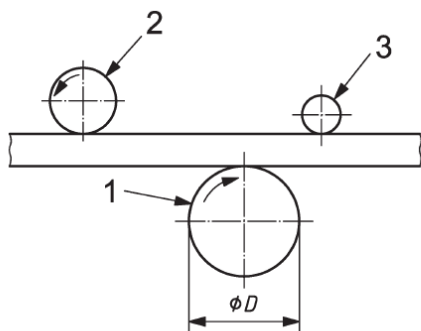


Fig. 6. Operational principle of the device for the bar bending and rebending [6]
1 – mandrel, 2 – support, 3 – carrier

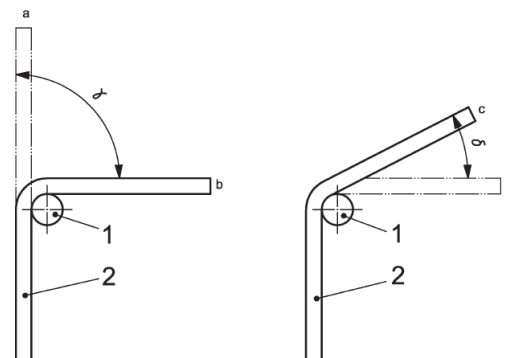


Fig. 7. Course of the bar rebend [6]
1 – mandrel, 2 – test piece,
a – initial position, b – position after bend test,
c – position after rebend test

The test piece is bend around the mandrel 1. Conditions of conducting the test (environmental temperature, angle of the test piece bending and the mandrel diameter) and the procedure of interpreting the results are determined in the product standards. If, as it is in the case of the reinforcement bars, detailed requirements related to the test results are not determined, then lack of cracks detected by

a person having normal or corrected eye sight, are regarded to be a proof that the bar test piece passed the bend test.

The procedure of rebending the bar consists of three stages: bending at the γ angle, artificial ageing and rebending at the δ angle. If the product standards do not determine the parameters, artificial ageing process of the test pieces, the following parameters are applied: heating to the temperature of 100°C , keeping the test piece in this temperature during $1\text{ h}^{+15\text{ min}}$, and then its cooling in motionless air to the environmental temperature. It is confirmed that the test piece passed the rebend test, if a person having normal or corrected eye sight does not notice any cracks on the test piece surface.

Fatigue test at an axial load consists in subjecting the test piece to a sinusoidal wave-form, varying cyclically. The test sample stays in the elastic state. Values F_{up} – maximum force, F_r – scope of the force variability and f – frequency of variables are determined in the product standards. The test is carried out till the test piece gets cracked or till the number of cycles without the test piece cracking, specified in the product standard, is achieved.

Innovative brands of construction materials are used more and more frequently both in the machine industry as well as in the building industry [11]. However, an implementation of new reinforcement steel grades, causes a necessity of additional tests of complete reinforced concrete elements. For example, testing a ductility impact of newly produced reinforcing steel on the wall of reinforced concrete elements is presented in [2]. The subject of tests includes reinforced concrete beams of a rectangular cross-section, whose reinforcement, both reinforcement bars as well as clevises are made of two grades of steel:

- newly produced steel S1 of high ductability – $A_{gt} \geq 8\%$, whose mechanical properties are obtained in the process of hot-rolling,
- steel S2, cold-rolled, whose strength properties are obtained through cold work.

Both steel grades are characterized by the strength in the yield point of $R_e=500\text{ MPa}$. A diagram of loading test beams is shown in Fig. 8.

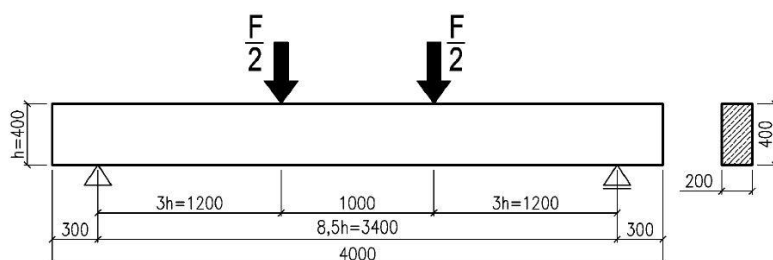


Fig. 8. Diagram of loading the test beam [2]

The tests were conducted until the beam damage. The following parameters were recorded: load value – F , beam deflection and a location of cracks crevices. A loss of the beam load-carrying capacity, due to shear, was connected with scratching the compressed zone of the beam cross-section as well as with bending out of clevises and in one case with a rapid break of both crevice arms. The test results confirmed a need of elaborating principles of applying crevices of the S1 steel in beams which can be damaged by shear [2].

The test methodology of adhesion forces of reinforcement bars to concrete in the case of test pieces, coming from the constructions withdrawn from use, are discussed in the work [12]. The tests were oriented onto an impact assessment of corrosion on the bar strength and onto a collection of data enabling an improvement of the method for assessing wear of reinforced concrete constructions.

2.3. Tests of composite reinforcement bars

Limited possibilities of using steel in disadvantageous environmental conditions forced a search of alternative solutions for concrete constructions. Among others, a high resistance to corrosion and changeable environmental conditions caused that non-metallic reinforcement mainly composite bars



GFRP (Glass Fiber Reinforced Polymer), BRFP (Basalt Fiber Reinforced Polymer) or CFRP (Carbon Fiber Reinforced Polymer) became an alternative for reinforcement steel [13]. Undoubted advantages of GFRP bars are: resistance to corrosion, lack of heat, electric and magnetic conduction, a small coefficient of thermal expansion along fibres, an early cuttability and a small density. In comparison with reinforcement bars disadvantages of GFRP bars include: lack of elastic reserve, small strength to shear, Young's modulus - 20÷30% of the Young's modulus of steel. A view of surfaces of exemplary GFRP and BFRP bars are presented in Fig. 9.



Fig. 9. View of surfaces of composite bars [8]
a) GFRP bar, b) BFRP bar

Testing of FRP bars is more difficult than testing of steel bars. Due to a small resistance of a composite to transverse forces, it is not possible to fix the composite directly in the MTS machine jaws but it is indispensable to install special anchors. A diagram of the FRP bar test piece, prepared for tests is shown in Fig. 10.

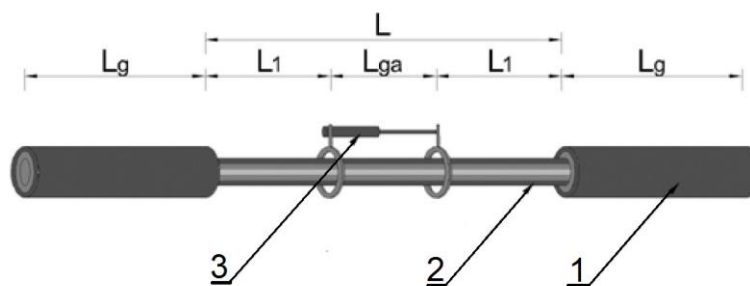


Fig. 10. Diagram of a sample prepared for testing [14]
1 – anchor, 2 – FRP, 3 – extensionmeter

Values of characteristic geometric dimensions of the sample, marked in Fig. 10, depend on the applied standard requirements [13].

Although for more than two decades FRP bars have been available on the market in the USA and Canada, so far there have been no verified methods of quality control of their production (QC) [15]. Generally speaking, the tests of FRP bars are related to well-known methods of testing steel bars. Up till the present time, a standard concerning the FRP bars has not been elaborated. However, they can be approved for an application, using technical approvals edited by the Building Research Institute (Instytut Techniki Budowlanej) [16] and the Road and Bridge Research Institute (Instytut Badania Dróg i Mostów) [17, 18]. In scientific investigations, conducted both in Poland [7, 8, 14], as well as abroad [19, 20], the recommendations of the ISO standards 10406 [21] and ACI 440.3R [22], embracing all the

basic experimental tests, are mainly applied. For example, diagrams of test methods of GFRP bars, included in the American Standard [22] are presented in Fig. 11.

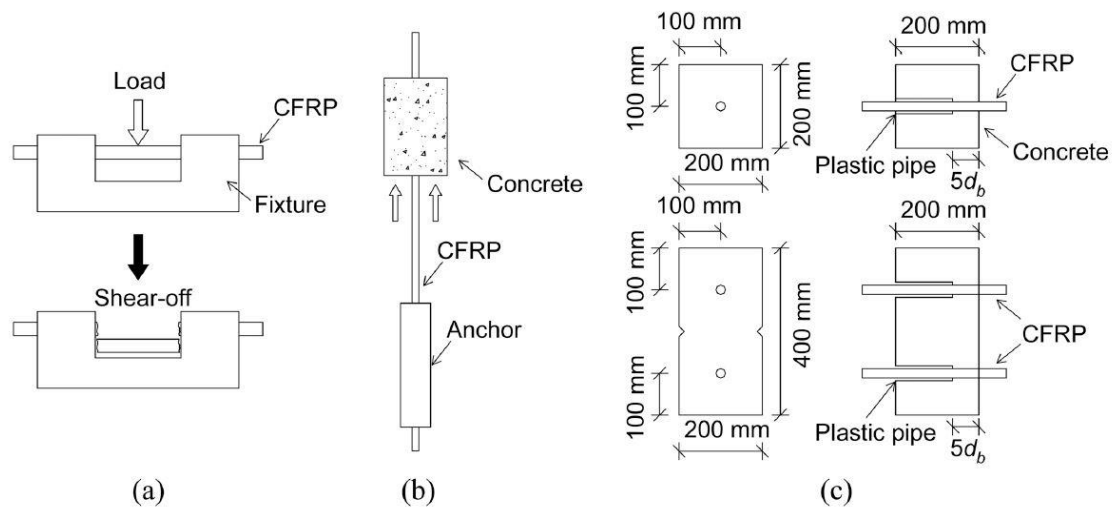


Fig. 11. Various test methods [19]
(a) – transverse shear, (b) – pullout, (c) – bond strength

It should be highlighted that mechanical properties, determined during the test, do not refer to a given type of FRP, but to the bar of the nominal diameter under testing. Mechanical properties of the bar depend not only on a content of fibres in the bar resin matrix but also on the method of finishing its surface (single-stranded, cross-stranded plait, mineral powder etc.)

As the results always refer only to the type of bar of a determined diameter subject to testing, so it is indispensable to obtain information from the producer about the strength properties of the applied FRP bar [13] at the stage of designing beam elements reinforced with FRP bars.

3. Results

Discussed test examples of reinforcing elements of reinforced concrete beams have been analyzed in the aspect of expanding the scope of tests realized at the KOMAG Laboratory of Tests.

At present in the case of standard tests of steel reinforcement bars, mentioned in [5] and [6], there is a possibility to conduct tests for tension, bending and rebending of a bar. In this scope the Laboratory possesses indispensable testing infrastructure and a realization of tests according to an external client's order is possible without any need for undertaking additional preparatory activities.

There is also a possibility of conducting tests of strength properties of complete reinforced concrete beams. The rig for testing kinematics of powered roof support units can be used for applying external load of the value up to 10 MN, to the beam of the length up to 7.5 m subject to tests. The mentioned test rig has already been used for testing building elements [23].

A commencement of adhesion tests of reinforcement bars to concrete requires separate preparations. It mainly concerns a preparation of anchors for the FRP test piece ends.

Although the tests of composite reinforcement bars [19] are conducted similarly to the tests of steel bars, but a specificity of these tests and lack of the Polish standard concerning the tests of FRP bars cause a necessity of elaborating specific testing procedures by the Laboratory.

4. Conclusions

An extension of the scope of services, offered by the Laboratory, including tests for other branches of economy, is usually connected with a need of undertaking a series of activities, both of formal-and-legal character as well as of technical character. In the case of testing bars for reinforcing and

prestressing concrete structures, discussed in this publication, special additional technical activities are connected with conducting adhesion tests of a reinforcement bar to concrete and with a preparation of test pieces of composite reinforcement bars for tests.

It would be also recommended to start research work oriented onto an elaboration of the Polish standard concerning tests of mechanical properties of composite reinforcement bars.

References

- [1] Ustawa o wyrobach budowlanych z dnia 16.04.2004 (Construction Products Law of 16.04.2004), Dz. U. z 2021 r. poz. 1213
- [2] Lorkowski Ł.: Badanie wpływu ciągliwości stali zbrojeniowej na ścinanie elementów żelbetowych. [Influence of reinforcing steel ductility on shear of reinforced structures]. In: Proceedings of the XXIII Naukowo - techniczna konferencja "Awaryjne Budowlane 2007" (XXIII Scientific and Technical Conference "Building Accidents 2007"). pp.993-1004
- [3] Rozporządzenie Ministra Infrastruktury i Budownictwa z dnia 23.12.2015 w sprawie próbek wyrobów budowlanych wprowadzanych do obrotu lub udostępniania na rynku krajowym (The Regulation of the Minister of Infrastructure and Construction of 23.12.2015 on samples of construction products placed on the market or made accessible on the domestic market), Dz. U. z 2020., poz.1508
- [4] Sprawozdanie z badań nr 64/DLB/2022 – dokumentacja wewnętrzna Laboratorium badań ITG KOMAG, (Research report no. 64/DLB/2022 – internal documentation of the KOMAG Research Laboratory) (unpublished)
- [5] PN-EN 10080:2007 Stal do zbrojenia betonu – Spajalna stal zbrojeniowa – Postanowienia ogólne (Steel for the reinforcement of concrete – Weldable reinforcing steel – General)
- [6] PN-EN ISO 15630-1:2019-04 Stal do zbrojenia i sprężania betonu – Metody badań Część 1: Pręty, walcówka i drut do zbrojenia betonu (Steel for the reinforcement and prestressing of concrete – Test methods – Part 1: Reinforcing bars, rods and wire)
- [7] Rajczyk M., Stachecki B.: Eksperymentalne badania przyczepności kompozytowego zbrojenia bazaltowego (BFRP) do betonu (Experimental studies of adhesion of composite basalt reinforcement (BFRP) to concrete). Zeszyty Naukowe Politechniki Częstochowskiej nr 24 (2018), pp. 305–312. doi:10.17512/znb.2018.1.48
- [8] Szymczak P.: Badanie przyczepności prętów kompozytowych GFRP oraz BFRP do betonu (Testing the adhesion of GFRP and BFRP composite bars to concrete). Przegląd Budowlany (Builders Review) 2/2018, pp. 36-39
- [9] Chu S.H., Kwan A.K.H.: A new method for pull out test of reinforcing bars in plain and fiber reinforced concrete. Engineering Structures Vol 164, 1 June 2018, pp. 82-91, doi.org/10.1016/j.engstruct.2018.02.080
- [10] Mousavi S.S., Dehestani M., Mousavi K.K.: Bond strength and development length of steel bar in unconfined self-consolidating concrete. Engineering Structures 2017; 131: 587-598
- [11] Krenicky T.: Manufacturing Technologies: Materials, operations and Applications. Tech Publications Ltd. 2017
- [12] Lundgren K., Robuschi S., Zandi K.: Methodology for Testing Rebar-Concrete Bond in Specimens from Decommissioned Structures. Int J Concr Struct Mater, 2019, pp. 13-38 doi.org/10.1186/s40069-019-0350-3
- [13] Jarek B., Kubik A.: Zastosowanie prętów zbrojeniowych z włókna szklanego (GFRP) w budownictwie (The use of glass fiber reinforcing bars (GFRP) in construction). Przegląd Budowlany (Builders Review) 12/2015, pp. 21-26
- [14] Szymczak P.: Badania fizycznych i wytrzymałościowych właściwości kompozytowych prętów zbrojeniowych w świetle norm (Investigations of physical and strength properties of composite reinforcing bars in the light of standards). Przegląd Budowlany (Builders Review) 6/2017, pp. 51-55
- [15] Echeverria L., Emparanza A. R., Nanni A., De Caso y Basalo F.: Quality Control Methodology for Composite FRP Rebars. Fifth International Conference on Sustainable Construction Materials and Technologies. (SCMT5) 14-17 July 2019 Kingston University, London conducted by Coventry University and Kingston University London. doi:10.18552/2019/IDSCMT5147



- [16] AT-15–9516/2015 Aprobata Techniczna ITB Pręty kompozytowe ARMASTEK do zbrojenia betonu, czerwiec 2015 (Technical Approval ITB. ARMASTEK composite bars for concrete reinforcement, June 2015)
- [17] AT/2014–02–3038 Aprobata Techniczna IBDiM Pręty kompozytowe z włókien do zbrojenia betonu, luty 2014 (IBDiM Technical Approval. Fiber composite bars for concrete reinforcement, February 2014)
- [18] AT/2015–02–3140/1 Aprobata Techniczna IBDiM Pręty kompozytowe z włókien do zbrojenia betonu, marzec 2016 (IBDiM Technical Approval. Fiber composite bars for concrete reinforcement, March 2016)
- [19] Kim Yail J., Jung Woo-Tai, Kang Jae-Yoon, Park Jong-Sup.: Testing methods and design specifications for CFRP-prestressed concrete members: A review of current practices and case studies. *Case Studies in Construction Materials* 16, 2022, e00842, doi.org/10.1016/j.cscm. 2021.e00842
- [20] Kodur V., Venkatachari S., Matsagar V.A., Singh S.B.: Test Methods for Characterizing the Properties of Fiber-Reinforced Polymer Composites at Elevated Temperatures. *Polymers* 2022, 14, 1734, doi.org/10.3390/polym14091734
- [21] ISO 10406–1:2015 Fibre-reinforced polymer (FRP) reinforcement of concrete – Test methods – Part 1: FRP bars and grid
- [22] ACI 440.3R: 2004 Guide Test Methods for Fiber-Reinforced Polymers (FRPs) for Reinforcing or Strengthening Concrete Structures
- [23] Madejczyk W., Szweda S.: Implementation of non-standard tests at powered roof support testing stands in KOMAG IOP Conf. Series: Earth Environ. Sci. 261 012028. 2019



Determination of physical and mechanical properties of limestones used as marble in Tut-Adiyaman Region in Turkey

Received: 08.08.2022

Accepted: 01.09.2022

Published online: 11.10.2022

Author's affiliations and addresses:

¹ Kahramanmaraş Sütçü İmam University, Department of Geological Engineering, Avşar Kampüsü, TR-46100 Kahramanmaraş, Turkey

* Correspondence:

e-mail: tamerrizaoglu@gmail.com

Tamer RIZAOĞLU ^{1*}, Canberk ÇOŞKUN ¹,
Murat CAMUZCUOĞLU ¹

Abstract:

This study aimed to reveal the petrography and physical-mechanical properties of limestones, which have an important reserve and are used as marble, in Tut district of Adiyaman province, which is one of the important cities of southeast Anatolia. As a result of petrographic analysis of the rock known commercially as Emprador, it was determined that it is bioclastic limestone with abundant nummulite fossils. Density, dry and saturated unit weight, water absorption, surface roughness, abrasion resistance and uniaxial compressive strength tests were applied to determine the physical and mechanical properties of the limestones. According to the test results obtained, the density of the limestones, dry unit weight, saturated unit weight, water absorption by weight, water absorption by volume, average surface roughness, ten points roughness average, maximum roughness value, Böhme abrasion resistance and uniaxial compressive strength values were determined as 2.486 gr/cm³, 2.478 gr/cm³, 2.52 gr/cm³, 1.482%, 3.644%, 3.31 µm, 16.24 µm, 20.03 µm, 8.958 cm³/50cm² and 1004.03 kgf/cm² respectively. The results show that the limestones in and around Tut (Adiyaman) county can be used in large areas for decorative purposes, with their physical and mechanical properties, as well as their colour tone and the texture formed as a result of the calcite veins being shaped like a natural pattern.

Keywords: natural stone, marble, limestone, physico-mechanical tests



1. Introduction

Located in the Alpine-Himalayan mountain belt, Turkey hosts many natural stone resources of different origins, in different colours and textures. In Turkey, which has proven its continuity in the natural stone industry and has more than 250 different resources released to the market, the reserves are spread over a wide region. Considering the distribution of known resources by regions, 32% of them are located in the Aegean region, 26% in the Marmara region, 11% in the Central Anatolia region and the remaining part in the Mediterranean, Black Sea and Eastern Anatolia regions (Çelik et al. 2021).

The oldest products used by human beings as building materials throughout history are known as natural stones. Marble, on the other hand, is a building product that has emerged as a result of the use of natural stones in the construction sector, especially in different areas, and has an important place in this field throughout the world. Today, the term marble is used in two different senses. Scientifically, it is defined as a metamorphic rock formed as a result of metamorphism of rocks with calcium carbonate composition; In commercial terms, it is used for natural stones that can give blocks, can be cut and processed and hold a good polish. Marbles, which provide a wide area of use in the field of construction, are required to have some physical and mechanical properties according to the area of their use. Today, marbles are widely used in kitchen work surfaces, stair steps, flooring, wall coverings and decorative purposes. As a result of the developing technology and methods, the marble sector has taken place of an industry branch that is growing day by day all over the world.

There are many studies in the literature on a determination of physical and mechanical properties of marbles, their extraction methods and positive and negative properties, as well as usability as raw materials. In this context, some researchers have carried out studies to determine the physical and mechanical properties of rocks of different origins and their usability as marble according to standards or to determine the properties of rocks currently used as marble [Erguvanlı et al. 1972; Onargan et al. 1995; Yavuz et al 2002; Çavumirza et al. 2003; Kılıç et al. 2003; Sümer et al. 2003; Tutuş and Kılıç 2007; Mutluhan and Özsan 2010; Kuşçu and Demiray 2015; Kılıç et al. 2018; Şimşek and Bilir 2022]. Some researchers have studied the usability of marble as a raw material in building materials such as artificial marble, concrete and gas concrete, and the usability of waste marble dust in similar building materials [Konak et al. 1999; Gülan et al.2016; Günaydın et al. 2016; Şimşek and Demir 2021]. Some researchers conducted studies on the performance analysis of marble cutting methods in quarries [Eleren and Ersoy 2007; Tolouei 2017; Çalışkan and Yavuz 2019; Dilmaç and Görgülü 2019].

Emprador type marbles (limestones) obtained from the marble quarry belonging to the Safvan Marble Enterprise located around the Tut district of Adıyaman province, used within the scope of the research, are included in the formation, which was first defined as the Hoya formation by Sungurlu (1974). The Hoya formation consists of limestone and dolomitic limestone units and is defined as gray-off-white coloured, abundant fossiliferous (abundant algae), angular fractures, clay-filled, medium-thick bedded karst formations. The Hoya Formation is Eocene aged and outcrops in an area of approximately 25 km in length and 7 km in the north of Adıyaman province (Yıldırım, 2013). In this study, it was aimed to investigate the mineralogical, physical and mechanical properties of limestones that can be used as marble in Tut district of Adıyaman province..

2. Materials and Methods

The marble samples, used within the scope of the study, were obtained from the Safvan Marble quarry in the Tut district of Adıyaman (Fig. 1a). The petrographic analysis, density, water absorption value, surface abrasion value, surface roughness and compressive strength values were investigated by sizing the samples in accordance with the test standards. In order to determine the petrographic analysis density, water absorption value, surface abrasion value, surface roughness and compressive strength values of the samples, they were cut in accordance with the standards (Fig. 1b).





Fig. 1 a) View of the study area, b) Samples sized for analysis

For petrography studies of the samples (limestone), thin sections were prepared in the thin section laboratory of the Mersin University, Faculty of Engineering, Department of Geological Engineering and analyzed under polarized microscope.

The density of the samples was determined by calculating the volume of the samples obtained from the field and not subjected to any treatment by water overflow method. In order to determine the dry and saturated unit weight and water absorption values, the dry weights of the samples were calculated by keeping them in an oven at 105°C until the maximum dryness was reached. Then, the same samples were kept in a container filled with water until they were completely saturated, and their saturation weights were calculated. As a result of substituting the obtained data in the relevant formulas, unit volume weight and water absorption values were determined (Fig. 2).

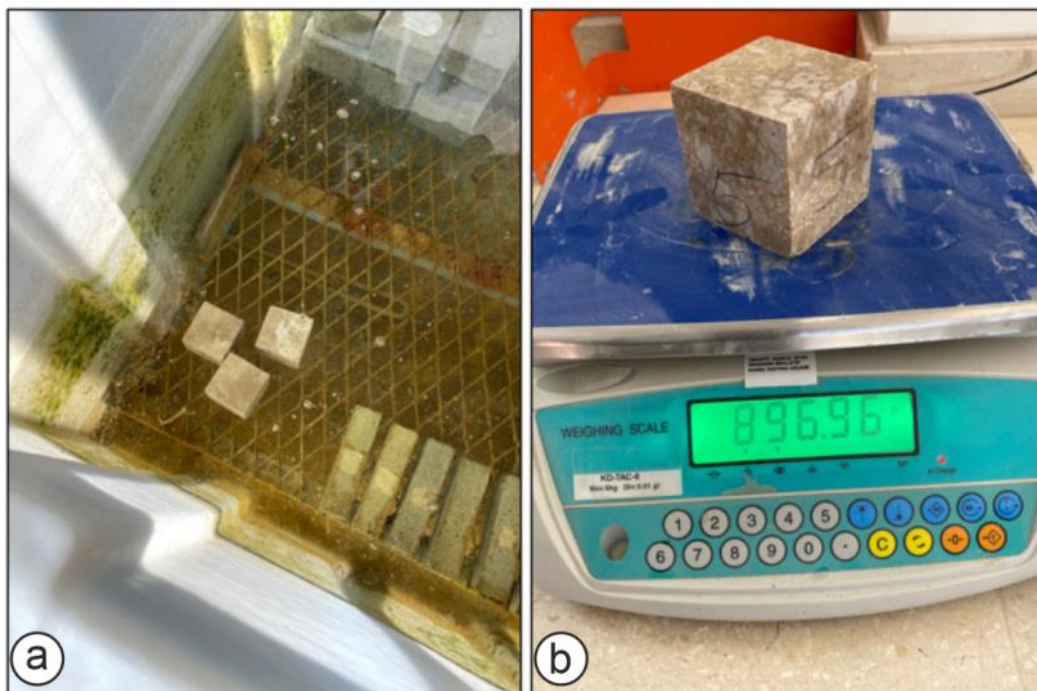


Fig. 2. Water absorption and dry-saturated unit weight measurement:
a) water tank, b) weight measurement

Marsurf M 300 diamond needle scanning surface roughness measuring device was used to determine the surface roughness of the marbles (Fig. 3). These measurements were applied taking into account the issues specified in the relevant standard. At least 5 different readings were made on each test sample and the average value was given. This measurement was related to the indentations and

protrusions on the sample surface as a result of the up and down movement of the 5 μm diameter diamond needle tip on the sample surface.



Fig. 3. Determination of surface roughness

In order to determine the compressive strength of the marbles, the samples cut to size in accordance with the marble standard were subjected to uniaxial compressive strength (Fig. 4). In order to determine the strength, measurements were made on 5 different samples and the average value was given.



Fig. 4. Determination of compressive strength: a) test application b) broken sample

Böhme abrasion test was used to determine the wear value on the surfaces of the marble samples (Fig. 5). For this test, the edge lengths of the samples were cut to 71 ± 1.5 mm and applied to the surface of each sample with 4 cycles and 88 cycles. The test was performed at least 3 times for each sample and the average of these values was given as volumetric loss.

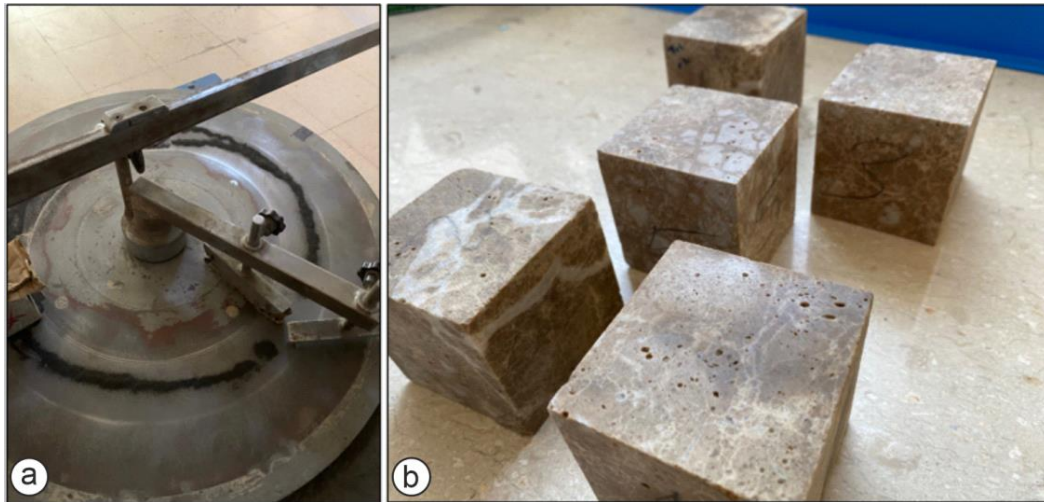


Fig. 5. Determination of Böhme abrasion resistance:
a) Böhme abrasion test instrument b) test samples

3. Results and discussion

Within the scope of the study, marble (limestone), known as Emprador in the marble sector, has been mined industrially in the region in recent years, making a great contribution to the regional economy. The produced marbles have various commercial names (Dark-Emprador, Adiyaman Emprador etc.). In the petrography study, carried out on limestones (Emprador marble) taken within the study area, according to the limestone classification made with the Folk (1965) classification; It was defined as bioclastic limestone and fossils and shell fragments of nummulites were observed in it (Fig. 6 b). It is known that the nummulites represent Eocene age, and the limestones sampled from the study area were found to be of Eocene age.

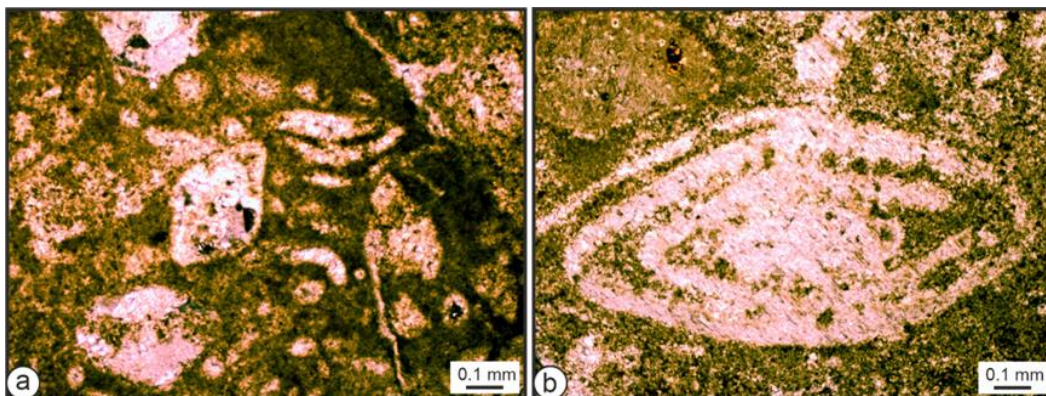


Fig. 6. Thin section images of Adiyaman (Emprador) limestone (Crossed Polarized Light):
a) Bioclastic limestone with nummulite fossils and various shell fragments,
b) Nummulite fossil thin section view

Density, dry-saturated unit weight, water absorption, uniaxial compressive strength, surface roughness and Böhme abrasion resistance tests were repeated at least 5 times for each test in order to determine the physical and mechanical properties of marbles within the scope of the tests presented as the mean of the data.

Table 1. Analysis Results of Marbles

Uygulanan Analiz	Ortalama Değer
Density (gr/cm ³)	2.486
Dry Unit Volume Weight (gr/cm ³)	2.478
Saturated Unit Volume Weight (gr/cm ³)	2.52
Water absorption by weight (%)	1.482
Water absorption by volume(%)	3.644
Böhme Abrasion Resistance (cm ³ /50cm ²)	8.958
Uniaxial Compressive Strength (kgf/cm ²)	1004.03
Average Surface Roughness (µm)	3.31
Ten Points Surface Roughness (µm)	16.24
Biggest Roughness Value (µm)	20.03

The density of the marbles used in the study was determined as 2.486 gr/cm³. According to TS 1910, the density of natural stone used as paving stone in buildings should be at least 2.55 gr/cm³ (TSE 1977a). The dry and saturated unit weights of the marbles were calculated as 2.478 and 2.52 gr/cm³, respectively.

The lower the water absorption value of the natural stone to be used in exterior cladding, the more ideal it is. The water absorption values of the rocks used in the study were determined as 1.482% and 3.644% by weight and volume, respectively. According to TS 1910, the water absorption value of natural stone should be at most 0.75% under atmospheric factors. According to TS 2513, the weight water absorption rate of natural building blocks should not be greater than 1.8% (TSE 1977b). According to TS 10449, the water absorption of marbles at atmospheric pressure should be less than 0.4% (TSE 2004). According to the results obtained, it is seen that Adıyaman limestones are suitable for use according to TS 2513.

According to TS 10449, the compressive strength of the marbles should be greater than 50 MPa for the marbles to be used in flooring, stair steps and flooring, and more than 30 MPa for the marbles to be used for wall covering. According to the results obtained, this value was determined as 1004.03 kgf/cm (98.462 MPa) in Adıyaman limestones. Therefore, the test samples are suitable to be used according to the relevant standards. When the Böhme abrasion resistance was examined, the abrasion of the limestone sample was found to be 8.958 (cm³/50cm²). According to TS 10499, this value is required to be less than 25 for natural stone used as paving stone and less than 15 for natural stone to be used in flooring. It is seen that the limestones used in the study meet both standard values.

4. Conclusions

As conclusions,

- Emprador marble (limestone) taken from the quarry of the Safvan Marble Enterprise in the Tut district of Adıyaman within the study area was determined to be bioclastic limestone containing abundant nummulite fossils as a result of the petrographic study.
- As a result, considering the tests performed on the limestones used in the study and the values required in the relevant standards, the density and unit volume weight values cannot meet the desired values in the relevant standards; uniaxial compressive strength, water absorption and Böhme abrasion resistance values were found to be above the required values.
- When all these tests are evaluated in general, it can be concluded that the examined limestones meet the building stone standards and are suitable for use.



Acknowledgements

The authors thank Osman Yıldırım, the manager of Safvan Marble Enterprise, who assisted in the procurement and sizing of Emprador marble from the quarry; Assoc. Dr. To Yağız Ferhat Özdemir for providing the surface roughness test, Prof.Dr. Hüseyin Temiz for allowing to use of the facilities of KSU Civil Engineering Department and Technician Samet Salar from Mersin University Geological Engineering Department for making thin sections of the rock.

References

- [1] Çalışkan M. A., Yavuz H.: Mermer Ocaklarında Kullanılan Zincirli Kesme Makinelerinin Performansının Araştırılması. Süleyman Demirel Üniversitesi Fen Bilimleri Enstitüsü Dergisi, 2019, 23, 108-118
- [2] Çavumirza M., Kılıç Ö., Mesut A.: Mucur (Kırşehir) Yöresi Kireçtaşı Mermerleri Ve Travertenlerinin Fiziko-Mekanik Özellikleri. Türkiyeiv. Mermer Sempozyumu (Mersem'2003) Bildiriler Kitabı 18-19, Aralık 2003
- [3] Çelik H., Alperen A. N., Bağcı M.: Sivaslı (Uşak) Yöresi Mermer Ocaklarındaki Doğal Taşların Teknolojik Ve Mineralojik-Petrografik Özelliklerinin Araştırılması. Proceedings Book, 10, 2021
- [4] Dilmaç M. K., Görgülü K.: Elmaslı Tel İle Mermer Üretiminde Basamak Geometrisinin Kesme Performansı Üzerine Etkileri. Avrupa Bilim Ve Teknoloji Dergisi, 2019, (17), 663-675
- [5] Eleren, A., and Ersoy, M. (2007). Mermer Blok Kesim Yöntemlerinin Bulanık Topsıs Yöntemiyle Değerlendirilmesi. Bilimsel Madencilik Dergisi, 46(3), 9-22
- [6] Erguvanlı K., Yüzer E., Güleç K., Zambak C.: Türkiye Mermerlerinin Fiziko-Mekanik Özellikleri Ve Mermerlerin Sınıflandırılmaları Hakkında Düşünceler. Türkiye Jeoloji Bülteni, 15(2), 153-170, 1972
- [7] Folk R.L.: Some aspects of recrystallization in ancient limestones: in Pray, L. C., and R. C. Murray (eds.), Dolomitization and Limestone Diagenesis, Soc. Econ. Paleont. and Mineral. Spec. Publ. 13, p. 14-48, 1965
- [8] Gülan L., Yıldız S., Keleştemur O.: Atık Mermer Tozu Ve Cam Lif Katkılı Betonun Mekanik Ve Fiziksel Özellikleri Üzerine Karbonatlaşmanın Etkisi. Fırat Üniversitesi Mühendislik Bilimleri Dergisi, 28(2), 2016, 189-200
- [9] Günaydın O., Güçlüer K., Ünal O.: Adıyaman Atık Mermer Tozlarının Gazbeton Üretiminde Kullanılabilirliğinin Araştırılması. Electronic Journal Of Construction Technologies/Yapı Teknolojileri Elektronik Dergisi, 2016, 12(1)
- [10] Kılıç A. M., Karakuş A., Keskin M. Ö.: Diyarbakır Yöresi Mermerlerinin Fiziko-Mekanik Özellikleri-Özgül Enerji İlişkisi. Türkiye Iv. Mermer Sempozyumu (Mersem '2003) Bildiriler Kitabı 18-19 Aralık 2003
- [11] Kılıç Ö., Kahraman E., Kılıç A. M.: Kireçtaşı Mermerlerinin Fiziko-Mekanik Özellikleri İle P Dalga Hızı Arasındaki İlişkinin İncelenmesi. Çukurova Üniversitesi Mühendislik-Mimarlık Fakültesi Dergisi, 2018, 33(2), 9-16
- [12] Konak G., Gürgeç S., Aksoy C. O., Küçük K.: Çok Kırıklı Mermer Sahalarının Agrega Olarak Kullanılabilirliğinin Teknik Açından İncelenmesi. 3. Endüstriyel Hammaddeler Sempozyumu /14-15 Ekim 1999, İzmir, Türkiye
- [13] Kuşçu M., Demiray Z.: Mermer Ve Yapıtaşı Olarak Kullanılan Farklı Jeolojik Kökenli Kayaçların Porozite, P-Dalga Hızı Ve Basınç Dayanımı İlişkisinin İncelenmesi. Süleyman Demirel Üniversitesi Fen Bilimleri Enstitüsü Dergisi, 2015, 19(2), 16-23
- [14] Mutluhan A., Özsan A.: Eskipazar Sarı Travertenleri İçin Kütleli Bozunma Ve Bozunma Sınıflaması. Jeoloji Mühendisliği Dergisi, 2010, 34(2), 113-132
- [15] Onargan T., Kızıl M. S., Köse H.: Ege Bölgesi Mermer Ve Yapıtaşları Potansiyeli Ve Değerlendirilmesi. Endüstriyel Hammaddeler Sempozyumu, Köse Ve Kızıl (Eds) © İzmir / Türkiye / 21-22 Nisan 1995
- [16] Sungurlu O.:VI. Bölge kuzey sahalarının jeolojisi, Türkiye 2. Petrol Kongresi Bildirileri. 22-25 Ocak 1974, Ankara. 85-107
- [17] Sümer E., Koçak K., Döyem A., Zedef V.: Burhan-Morcalı (Karaman) Mermerlerinin Fiziksel Ve Mekanik Özellikleri. Selçuk Üniversitesi Mühendislik-Mimarlık Fakültesi Dergisi, 2003, 18(1), 37-42



- [18] Şimşek O., Bilir M.: Haymana-Demirözü Mevki Mermerlerinin Fiziksel Ve Mekanik Özelliklerinin Belirlenmesi. . Ulusal Başkent Disiplinler Arası Bilimsel Çalışmalar Kongresi, Ankara, Türkiye, 21 - 22 Haziran 2022, Ss.83-88
- [19] Şimşek O., Demir, Ş.: Mermer Tozu Katkılı Lifli Betonun Fiziksel Ve Mekanik Özelliklerine Lif Tipi Ve Oranın Etkisi. Politeknik Dergisi, 1-1, 2021
- [20] Tolouei S.: Mermer Fabrikalarında Kullanılan Büyük Çaplı Dairesel Testerelelerin (S/T) Performans Analizi. Politeknik Dergisi, 2017, 20(3), 651-662
- [21] T.S.E., 1977a, “Kaplama Olarak Kullanılan Doğal Taşlar”, Ts 1910 Udk 691.215, Ankara
- [22] T.S.E., 1977b, “Doğal Yapı Taşları”, Ts 2513 Ics 91.100.15, Ankara
- [23] T.S.E. 2004, “Mermer-Kalsiyum Karbonat Esaslı-Yapı Ve Kaplama Taşı Olarak Kullanılan Tadil 1”, Ts 10449/T1, Ankara
- [24] Tutuş M., Kılıç A. M.: Çukurova Yöresinde Bulunan Bazı Mermerlere Ait Fiziko-Mekanik Özelliklerin İstatistiksel Analizi. Ç.Ü Fen Bilimleri Enstitüsü Yıl: 2008, Cilt: 17-8
- [25] Yavuz A. B., Türk N., Koca M.Y.: Muğla Yöresi Mermerlerinin. Mineralojik, Kimyasal Fiziksel Ve Mekanik Özellikleri. Jeoloji Mühendisliği Dergisi, 2002, 26(1), 1-18



<https://doi.org/10.32056/KOMAG2022.3.4>

Analysis of one-day forecasts of the maximum methane concentration in a tailgate of a longwall ventilated with U system - a case study

Received: 24.09.2022

Accepted: 03.10.2022

Published online: 11.10.2022

Author's affiliations and addresses:

Henryk BADURA  1*

¹ Silesian University of Technology
Professor Emeritus, Poland

* Correspondence:

e-mail: henryk_badura@o2.pl

Abstract:

Methane that is released into the mine atmosphere poses a threat to the miners working there. Methane at concentrations of 5-15% by volume in air is an explosive gas. It has caused devastating explosions in mines all over the world. Therefore, in methane mines, concentration of methane in the face and in the entire mine is controlled through well-designed ventilation system. This system controls concentration of methane in the mine atmosphere and in the rock mass as well as in the mine goafs. The article's main objective includes a presentation of a forecast for maximal methane concentration in the determined time interval. Sensors were installed in the gate draining the air from longwall: up to 10 m in front of the longwall and at the roadway exit. Both forecasts were made using prognostic equations, using the measurement data in the ventilation roadway of one of the longwalls at the JSW S.A. mine.

Keywords: methane, maximum methane concentration, methane concentration forecasts, methane concentration sensors



1. Introduction

Coal Mine Methane (CMM) is a gas released from coal seams and the surrounding rock layers.

Methane released into the atmosphere is a significant greenhouse gas contributing to climate change worldwide. Currently in the US it is assumed that the global warming potential (GWP) of methane is 25 times greater than that of carbon dioxide for 100 years [1]. However, the literature shows GWP values of 21, 23, 25 and even 28. The US Environmental Protection Agency (USEPA) estimates that methane from coal mines is responsible for 8% of global methane emissions caused by human activity [2].

Experience from the last 20 years shows that the most common methane GWP value is 72. The lifespan of methane in the atmosphere is estimated at about 7 years.

Methane released into the mine atmosphere poses a threat to the miners working in the mines. Methane at concentration 5-15% in air is explosive. In the long history of coal mining industry, methane has been the cause of devastating explosions in many mines around the world.

A one-day forecasts of the maximum concentration of methane in the sensors located in near-longwall roadway, which removes used air from the longwall: up to 10 m ahead of the longwall and at the roadway exit is presented.

2. Literature review

Methane explosion hazard is one of the most common threats in the Polish coal mining industry [3, 4]. The report prepared by the Mining Department of the State Mining Authority [5] for 2020, which presents data on methane and outburst hazards in Polish underground mining industry, shows that in 2020, 77.1% of coal production in Poland came from methane deposits. So far, the highest percentage of coal extracted from methane seams was in 2017 - 79.5%.

Methane in Polish coal deposits occurs in three forms [6, 7]:

- as free methane (in fractures, macropores and mesopores),
- coal bound methane (physical and chemical sorption),
- methane dissolved in water.

During the coal seam mining, methane flows into the mine atmosphere from the mined coal seam and from the roof and floor rocks. The carriers of methane in the floor and roof rocks are coal seams and layers that are not suitable for mining as well as porous waste rocks, mainly sandstones. In waste rocks, methane occurs almost entirely as free gas, not adsorbed. Mining exploitation causes the outflow of methane into the mine atmosphere from the mined seam and from the rocks surrounding it.

The method of ventilation of the longwall area has a significant impact on methane hazard and the distribution of methane concentration in workings [8, 9, 10, 11]. This publication concerns a ventilated longwall in the U system, i.e. the ventilation air stream flows from the ramp along the head entry towards the longwall, then ventilates the longwall and then, through the ventilation roadway, flows to the ramp. The direction of air flow in the head entry and tailgate are opposite. It is a typical method of ventilating the areas of non-methane and methane longwalls with low and medium methane content. The ventilation methane capacity, i.e. the stream of methane in the air stream in the longwall area, cannot exceed 20 m³CH₄/min [12]. If technical measures do not allow to obtain ventilation methane capacity not exceeding the above-mentioned level, it is necessary to use ventilation systems other than U, e.g. Y or W [13, 14].

In order to protect the personnel working in longwalls against the threats resulting from the presence of methane in the seam and surrounding rocks, a methane concentration should be forecast prior to the of exploitation of the seam in a given longwall. The forecast prepared at the Central Mining Institute in Katowice [15] is the most widely used in Poland, but other forecasts are also used. Many methods of methane concentration have been developed in the world. They are



adapted to the natural conditions of a specific coal basin. Examples can be found in the literature, e.g. [16-19].

In the Polish coal mining industry, the last thirty years have brought very significant changes in the equipment with telemetric systems for measuring physical and chemical parameters of the mine atmosphere [20, 21]. One of the functions of these systems in methane mines is the measurement of methane concentration in places specified by mining regulations. The system has a measuring, recording and archiving function, informing, warning and switching off the electric current. Due to the deeper understanding of the phenomenon of methane emission to workings, the function of recording and archiving measurement data in automatic measurement systems plays an essential role. These data can be derived outside the telemetry system and processed at any time, which allows for their comprehensive analysis and inference in order to better understand the methane emission phenomenon and use it to improve work safety in mining [22-24]. In highly methane longwalls, more sensors are used than required by law. Additional sensors are placed in the locations where increased methane concentrations may occur.

The article [24] describes a set of model parameters for one-day forecasts of the mean and maximum methane concentration at the outlet of the workings that discharge used air from the longwall. The research work conducted on applying these models to forecast the average methane concentration at the outlets from the longwall ventilation workings confirmed their accuracy [25, 26]. This article presents an attempt to use these models to forecast the maximum concentration of methane in a roadway discharging used air from the longwall, at the location of the methane concentration sensor at a distance of up to 10 m from the face of the longwall and at the exit of the ventilation roadway (10-15 m before the crossing with another workings with air supply). The air stream in these places is almost the same, however, the degree of homogeneity of the air-methane mixture at the exit of the roadway and at a distance of up to 10 m in front of the longwall is different. It is caused by turbulent air flow in the workings and the phenomenon of diffusion.

An important issue is demethanization, i.e. capturing methane directly from the rock mass and discharging it to the surface via a pipeline system. The negative pressure in this system is often caused by suction devices located on the surface. A large part of such methane is processed economically, e.g. to power electricity generators or to generate heat.

Proper management of methane from hard coal deposits will contribute to its economic use, and at the same time will reduce the greenhouse effect associated with the release of methane into the atmosphere [27, 28].

3. Materials and Methods

Data on methane concentration are archival data and come from automatic measurements of methane concentration in one of the longwalls of Jastrzębska Spółka Węglowa S.A.

Using the software of the methane concentration measuring system, the measurement data are converted into a text form and transfer out the measuring system in a tabular form (Table 1).

Table 1. Sample measurement data of methane concentration in one of the longwalls of JSW S.A.

Start time	Measurement	Duration	Statuses
12.04.2022 15:05:24	1.2%CH4	0:00:01	
12.04.2022 15:05:05	1.3%CH4	0:00:19	
12.04.2022 15:04:32	1.4%CH4	0:00:33	
12.04.2022 15:04:20	1.3%CH4	0:00:12	
12.04.2022 15:04:12	1.2%CH4	0:00:08	

In the above entry, in the first column of Table 1 (Start Time), the date of measurement and the start time of the measurement of methane concentration are recorded, with the value given in



the second column, entitled Measurement. Measured concentration in the Measurement column is given with an accuracy of 0.1%, which corresponds to the measurement accuracy of the methane sensor. The next column, Duration, defines the time of occurrence of the methane concentration with the value given in the previous column with an accuracy of 1 second. In the Status column, there are notes regarding extraordinary states, e.g. checking the accuracy of measurements, exceeding the set concentration threshold, etc.

On the basis of the data prepared in this way, using the PROGNET program developed at the Silesian University of Technology, the average, minimum and maximum values of methane concentration are calculated in a given day, with the day being counted from a given hour, not from 00:00:00. In the data contained in the presented article, the calculation day is the period from 06:00:00 on the current day to 06:00:00 on the following day.

With the output data prepared in such a way, the forecast values of methane concentration are calculated using the models presented in the paper [24].

4. Results – characteristics and interpretation of measurement data

The measurement data covers 195 days, with 194 one-day forecasts, as one-day forecast uses the measurement values of the previous day.

Fig. 1 shows maximum methane concentrations in a given day, calculated on the basis of the measurements of the sensor located in the ventilation roadway up to 10 m in front of the longwall and the sensor located 10-15 m before the exit from this roadway.

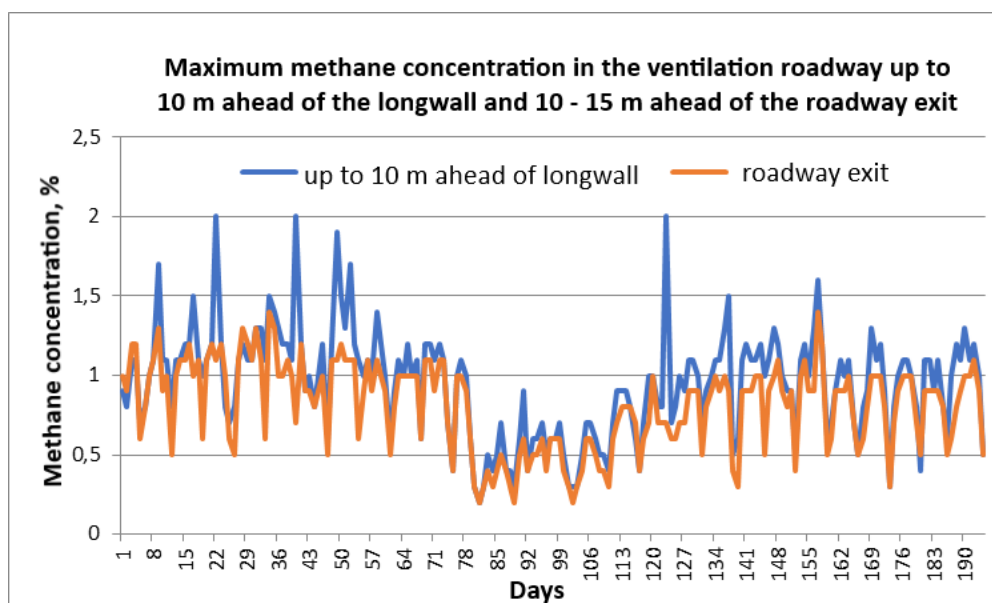


Fig. 1. Maximum measured methane concentration in the places where the sensors are located in the ventilation roadway

In Fig. 1 it can be seen that on most observation days the maximum concentration in the ventilation passage up to 10 m in front of the face of the wall is higher than at the exit of the ventilation roadway. Characteristic parameters of average methane concentrations found with sensors in the discussed places are presented in Table 2.

Table 2. Statistical parameters of the maximum concentrations of methane found in the ventilation pavement at a distance of 10 m in front of the wall and at the roadway exit, calculated for the entire observation period

Parameter	Up to 10 m ahead of longwall	At the roadway exit
average, %CH ₄	0.95	0.81
median, %CH ₄	1.00	0.90
percentile 0,9, %CH ₄	1.30	1.10
minimum, %CH ₄	0.20	0.20
maximum, % CH ₄	2.00	1.40
standard deviation, %CH ₄	0.34	0.28
variation factor, %	35.61	34.10
range of methane conc., %CH ₄	1.80	1.20
sum of max. conc., %CH ₄	184.10	157.60

Values of eight parameters of methane concentration calculated for the readings of the methane concentration sensor located up to 10 m in front of the longwall face are higher than at the exit of the ventilation roadway. And so the mean value is higher by 0.14%, the median by 0.10%, the 0.9 percentile by 0.20% CH₄, the maximum value by 0.6%, the range of methane concentration is greater by 0.6%, the standard deviation is greater by 0.06%, and the coefficient of variation in the methane concentration is greater by 1.51%

The standard deviation and the variation factor testify the high variability of the methane emission to mine workings related to coal seam mining.

Only the minimum values of the maximum concentrations of methane in both considered places are equal and amount to 0.2%.

The prognostic equations developed for the outlet from the ventilation roadway were used to predict the concentration of methane up to 10 m in front of the longwall. To assess whether these equations give satisfactory results, methane concentration at the exit of the roadway were also forecasted to compare the forecast results in both of places.

Fig. 2 and 3 show the graphs of the maximum measured and forecasted methane concentrations in both of the above-mentioned places, and Tables 3 and 4 contain their statistical parameters.

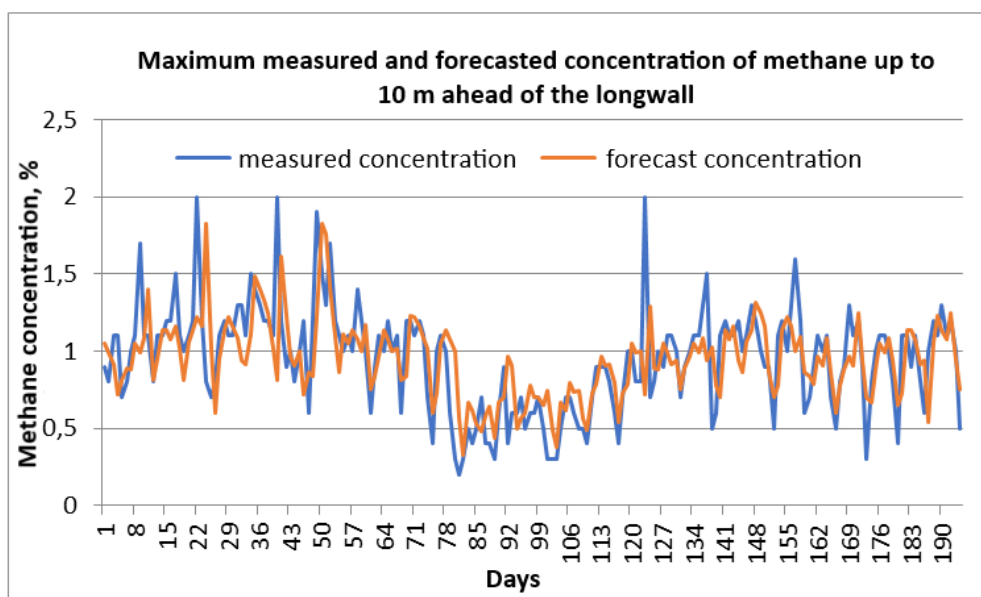


Fig. 2. Maximum measured and forecasted methane concentration in the tailgate at a distance of up to 10 m from the longwall face

Table 3. Statistical parameters of the maximum measured and forecast methane concentrations in the roadway within 10 m from the longwall face

Parameter	Up to 10 m ahead of longwall - measurement	Up to 10 m ahead of longwall - forecast	Difference
average, %CH ₄	0.95	0.95	0
median, %CH ₄	1.00	0.96	-0.04
percentile 0.9, %CH ₄	1.30	1.23	-0.07
minimum, %CH ₄	0.20	0.33	0.13
maximum, % CH ₄	2.00	1.83	-0.17
standard deviation, %CH ₄	0.34	0.25	-0.09
variation factor, %	35.61	26.22	-9.39
range of methane conc., %CH ₄	1.80	1.50	-0.30
sum of max. conc., %CH ₄	184.10	183.91	-0.19

The average maximum methane concentration, calculated on the basis of measurements taken over 194 days, is 0.95% CH₄, also calculated from the forecasts is 0.95% CH₄. However, this does not mean that all measured and forecast values are close to each other. The medians already differ, but the median calculated on the basis of the measurements is higher than the median calculated for the forecasts. The forecast has lower values of the following further statistical parameters: 0.9 percentile, maximum, standard deviation and coefficient of variation, methane concentration range. Only the projected minimum value is higher than the measurement value, which of course limits the variations range of the forecast maximum methane concentration (the measurement range of methane concentration variations was 1.8% CH₄, and the forecasted 1.5% CH₄). The sum of the maximum methane concentrations calculated on the basis of the measurements is also higher than the sum of the forecast maximum concentrations, although the difference is surprisingly small. The reduced range of variability of the forecasted maximum concentrations is also evidenced by the much lower value of the variation factor of the forecast methane concentrations (26.22%) in relation to the variation factor of the measured values of the maximum methane concentration (35.61%).

Nex the results of measurements and forecasts of the maximum concentration of methane at the exit of the ventilation roadway (10-15m ahead of the connection with another active roadway).

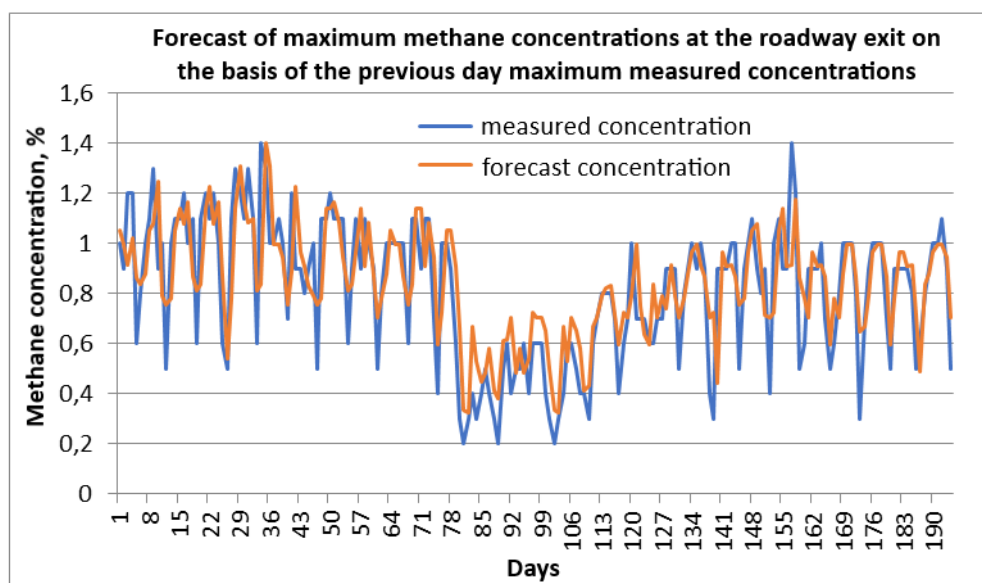
**Fig. 3.** Maximum measured and forecasted methane concentration in the tailgate at the roadway exit

Table 4. Statistical parameters of the maximum measured and forecasted methane concentration at the exit of the ventilation roadway

Parameter	At the roadway exit - measurement	At the roadway exit - forecast	Difference
average, %CH ₄	0.81	0.84	0.03
median, %CH ₄	0.90	0.86	-0.04
percentile 0.9, %CH ₄	1.10	1.14	0.04
minimum, %CH ₄	0.20	0.33	0.13
maximum, %CH ₄	1.40	1.40	0.00
standard deviation, %CH ₄	0.28	0.21	-0.07
variation factor, %	34.10	25.01	-9.09
range of methane conc., %CH ₄	1.20	1.07	-0.13
sum of max. conc., %CH ₄	157.60	163.32	5.72

Mean value of the maximum concentration of methane, calculated on the basis of measurements taken over 194 days, is 0.81% CH₄, while the calculated value based on prognostic equations is 0.84% CH₄, i.e. it is higher by 0.03% CH₄. The difference between the medians is -0.04% CH₄, i.e. the median of measurement data is higher. The difference between the 0.9 percentiles is 0.04%, which is not much overestimated in relation to the measured one. The minimum forecast value of the maximum methane concentration is by 0.13% higher than the measured value, and the maximum values do not differ. The standard deviation of the forecasts is lower than the standard deviation of the measurements by -0.07% CH₄, while the variation factor of the forecasts is lower than that calculated from measurements by -9.09%.

The forecasts have a slightly narrower range of variation in relation to the measurements, and the difference is -0.13% CH₄.

Taking into account the entire observation period of the prognostic parameters, it can be concluded that they do not differ much, and the forecast is slightly overestimated. The sum of the values of the forecast methane concentrations is 5.72% CH₄ higher than the sum of the measured values.

Table 5 presents differences between the measurement parameters and the projected maximum methane concentration in the ventilation pavement at a distance of up to 10 m in front of the wall and at the pavement outlet, at a distance of 10-15 m from the intersection with another excavation.

Table 5. Differences between the statistical parameters of the maximum methane concentration in the ventilation roadway up to 10 m ahead the longwall face of the and at a distance of 10-15 m from the intersection with another excavation

Parameter	Differences 10 m ahead the longwall	Differences from the intersection
average, %CH ₄	0	0.03
median, %CH ₄	-0.04	-0.04
percentile 0.9, %CH ₄	-0.07	0.04
minimum, %CH ₄	0.13	0.13
maximum, %CH ₄	-0.17	0.00
standard deviation, %CH ₄	-0.09	-0.07
variation factor, %	-9.39	-9.09
range of methane conc., %CH ₄	-0.30	-0.13

Negative values mean that the statistical parameters of the maximum methane concentration forecasts are lower than their values for the measured data.



The comparison of the measurement parameters and the forecast maximum methane concentration shows that the differences in both considered places are small, and therefore the forecast equations developed for the exit from the roadway may be helpful in practice for the assessment of the methane hazard in close proximity (up to 10 m) to the longwall exit to the ventilation roadway.

5. Conclusions

Possibility of using the models for one-day maximum methane concentration forecast, developed for the ventilation roadway outlet to forecast the maximum concentration of methane in the given roadway at the location of the methane concentration sensor at a distance of up to 10 m from the face of the longwall was presented. The parameters of the forecast models were taken from paper [24]. Comparison of the statistical parameters concerning the forecasts of methane concentration in the above-mentioned places shows that the accuracy of the forecasts of the maximum methane concentrations in both places are similar, with a slightly greater error in the forecast of methane concentration in the roadway at a distance of up to 10 m ahead of the longwall. Further research work to analyze methane concentration forecasts at the longwall outlet using the forecast equations, presented in paper [24], enabled their practical use as well as development of new forecast functions regarding the maximum concentration of methane in the roadway, in the immediate vicinity of the outlet from the longwall.

References

- [1] IPCC (Intergovernmental Panel on Climate Change), 2007. Climate change 2007: The physical scientific basis. Cambridge, UK: Cambridge University Press, 2007. web site: <http://www.ipcc.ch/pdf/assessment-report/ar4/wg1/ar4-wg1-chapter2.pdf> [accessed: 22.08.2022]
- [2] USEPA, 2012. Global Anthropogenic Non-CO2 Greenhouse Gas Emissions: 1990-2030. EPA Report 430-S-12-002, December 2012 Revised. https://www.epa.gov/sites/default/files/2016-08/documents/summary_global_nonco2_projections_dec2012.pdf [accessed: 22.08.2022]
- [3] Mirek A., Katan D.: Zagrożenie metanowe w polskim górnictwie węgla kamiennego w ostatnim dwudziestolecu i perspektywy kształtowania się poziomu tego zagrożenia w najbliższych latach. Materiały Szkoły Eksploatacji Podziemnej. Kraków, 2013.
- [4] Roszkowski J., Szlązak J., Szlązak N.: Zagrożenie metanowe w kopalniach węgla kamiennego. Materiały I Szkoły Aerologii Górniczej. Wydawnictwo Centrum Elektryfikacji i Automatykacji Górniczej EMAG w Katowicach. Zakopane, 1999
- [5] Ocena stanu bezpieczeństwa pracy, ratownictwa górniczego oraz bezpieczeństwa powszechnego w związku z działalnością górnictwo-geologiczną w 2020 roku. Wyższy Urząd Górniczy. Katowice, 2021
- [6] Kozłowski B., Grębski Z.: Odmetanowanie górotworu w kopalniach. Wydawnictwo „Śląsk”. Katowice, 1982
- [7] Układ węgiel kamienny – metan w aspekcie desorpcji i odzyskiwania metanu w wyrobiskach kopalnianych. Praca zbiorowa pod redakcją M. Żyły. Nauka i Technika Górnicza. Uczelniane Wydawnictwo Naukowo-Dydaktyczne AGH. Kraków, 2000
- [8] Frączek R.: Zwalczanie zagrożenia metanowego w kopalniach węgla kamiennego. Gliwice, 2005
- [9] Badura H., Jakubów A., Klamecki A.: Application of Statistic Predictions for Evaluation of Methane Inflow. New Challengers and Visions for Mining. Methane Treatment. Issued by Foundation for the AGH – University of Science & Technology. Kraków, 2008
- [10] Grubengasbekaempfung im Hohleleistungsstreb. Praca zbiorowa pod redakcją K. Noacka. Steinkohlenbergbauverein. Essen 1977
- [11] Krause E., Łukowicz K., Gruszka A.: Zasady przewietrzania wyrobisk górniczych w warunkach zagrożenia metanowego wraz z doбором urządzeń wentylacyjnych dla jego zwalczania. Wydawnictwo GIG. Katowice-Mikołów, 2004
- [12] Rozporządzenie Ministra Energii z dnia 23 listopada 2016 r. Dziennik Ustaw RP. Poz.1118. Warszawa, 09.06.2017 r.



- [13] Frycz A., Szlązak J.: Wpływ rozcinki złoża w pokładach metanowych na występowanie metanu w rejonie ściany. Przegląd Górniczy nr 2, 1977
- [14] Szlązak J., Szlązak N.: Ocena systemów przewietrzania wyrobisk ścianowych w kopalniach węgla kamiennego w warunkach zagrożenia metanowego i pożarowego. Materiały 3 Szkoły Aerologii Górniczej. Wydawnictwo Centrum Elektryfikacji i Automatykacji Górnictwa EMAG w Katowicach. Zakopane, 2004
- [15] Krause E., Łukowicz K.: Dynamiczna prognoza metanowości bezwzględnej ścian (Poradnik techniczny). Główny Instytut Górnictwa. Kopalnia Doświadczalna Barbara w Mikołowie. Katowice – Mikołów. 2000
- [16] Dahar B.B., Singh A.K., Singh H., Kispotta J.: Prediction of methane emission in longwall workings. 27th International Confer. of Safety in Mines Research Institute. New Delhi. 1997
- [17] Dixon D.W., Longson I.: A statistical method for methane prediction and improved environmental control. Proceedings of the 6th US mine Ventilation Symposium. 1993
- [18] Katoro Ohega, Sohei Shimada: Gas emission prediction and control in deep coal mines. Mineral Resources Engineering. Vol. 9, No. 2. 2000
- [19] Lunarzewski L.W., Lunarzewski A.L., Pilcher R.C.: A new approach to predicting underground gassiness for gas capture and ventilation system. Proceedings of the 7th US Mine Ventilation Symposium 1995
- [20] Cierpisz S., Miśkiewicz K., Musioł K., Wojaczek A.: Systemy gazometryczne w górnictwie. Monografia. Wydawnictwo Politechniki Śląskiej. Gliwice, 2007
- [21] Wasilewski S.: Zintegrowany system kontroli zagrożeń metanowo – pożarowych. Mechanizacja i Automatykacja Górnictwa. 1994
- [22] Badura H.: Zastosowanie szeregów czasowych do prognoz krótkoterminowych metanowości. Zeszyty Naukowe politechniki Śląskiej, seria Górnictwo, z. 250. Gliwice, 2001
- [23] Badura H., Stabla H., Plewa F.: Dyspozytorski program do bieżącej oceny i prognozy zagrożenia metanowego jako narzędzie do wspomagania doboru środków profilaktyki metanowej. Materiały Szkoły Eksploatacji Podziemnej 2013. Instytut Gospodarki Surowcami Mineralnymi i Energią PAN. Katedra Górnictwa Podziemnego AGH. Kraków, 18-22 lutego 2013
- [24] Badura H.: Metody prognoz krótkoterminowych stężenia metanu na wylotach z rejonów ścian zawałowych w kopalniach węgla kamiennego. Monografia. Wydawnictwo Politechniki Śląskiej. Gliwice, 2013
- [25] Niewiadomski A.P., Badura H.: Evaluation of a one-day average methane concentrations forecast at the outlet from the longwall ventilation region as tool of supporting selection of methane prevention measures. Topical issues of rational use of natural resources 2019. London: Taylor & Francis Group, 2019
- [26] Niewiadomski A.P., Badura H., Pach G. Recommendations for methane prognostics and adjustment of short-term prevention measures based on methane hazard levels in coal mine longwalls. E3S Web of Conferences 266, art. no. 08001, 2021
- [27] Łukaszczyk Z.: Pozyskiwanie i gospodarcze wykorzystanie metanu ze zlikwidowanych kopalń węgla kamiennego. Monografia. Wydawnictwo Politechniki Śląskiej. Gliwice. 2019
- [28] Łukaszczyk Z., Nawrat S., Badura H.: Emisja metanu z kopalń do atmosfery i możliwości jego proekologicznej utylizacji. Wydawnictwo IGSMiE PAN. Kraków, 2022



<https://doi.org/10.32056/KOMAG2022.3.5>

Use of the iLogic Autodesk Inventor tool in the process of designing self-propelled drilling rigs

Received: 01.09.2022

Accepted: 04.10.2022

Published online: 11.10.2022

Author's affiliations and addresses:

Lukasz BOŁOZ  ^{1*}

¹ AGH University of Science and Technology, Faculty of Mechanical Engineering and Robotics, Department of Machinery Engineering and Transport, al. Mickiewicza 30, 30-059 Krakow, Poland

* Correspondence:

e-mail: boloz@agh.edu.pl

Abstract:

In the article, a practical example of using the Autodesk Inventor Professional iLogic tool for designing self-propelled drilling rigs has been presented. Self-propelled drilling rigs are advanced mining machines with a complex structure. At the design stage, most of the structural changes affect the stability, manoeuvrability and coverage area of the machine. Working on detailed machine models is time-consuming and unnecessary in the initial phase of the project. Therefore, a parametric 3D model of a two-boom drilling rig has been developed. It enables a quick analysis of selected machine properties depending on a number of significant parameters. The most important dimensions, masses and centres of gravity of each subassembly are entered by transparent editing windows. Next, model tests are carried out taking into account the pass through a face end of a given width as well as the coverage area of a face with specific dimensions. At each stage of model tests, the location of the machine's centre of gravity against the stability triangle background is analysed. In addition, the model allows entering the longitudinal and transverse angles of inclination of the working as well as determining the distance of the centre of gravity from the tipping edge. The model is a practical tool that makes it possible to easily determine the inner and outer turning radius as well as the working area of the machine while constantly controlling its stability. Due to the use of simplified geometry of subassemblies, the changes in parameters result in an instantaneous change of the model and allow a quick analysis of their impact.

Keywords: self-propelled drilling rigs, machine stability, parametric modelling, iLogic, Autodesk Inventor Professional



1. Introduction

Self-propelled mining machines are the machines commonly used in many underground mines. These machines work in the mining of metal ores, precious stones or salt. Changing in working conditions and growing customer expectations force constant changes. For many years, there has been a demand for advanced control systems, including automation and diagnostics as well as remote operation. In recent years, the first battery-powered machines have also appeared. Advanced, closed and air-conditioned operator's cabins are increasingly used. Rapid changes and small-lot or almost one-off manufacture require quick and efficient designing process. Manufactured machines, often prototypes, are almost immediately intended for operation in the mine. Any design or assembly errors are unacceptable and entail financial implications. Advanced CAX programs, supporting the design work, satisfy the high demands of the current market. CAD (Computer Aided Design) and CAE (Computer Aided Engineering) are the essential programs used by the designers on daily basis.

CAD programs, such as Catia, NX, Creo, Inventor, support design work, including parametric design. CAD programs often have CAE components allowing to analyse load or strength [1, 2]. CAX programs are powerful tools with great possibilities. Numerical methods of solving physical models concern various issues, not only the strength of materials and kinematic and dynamic simulations, but also the analysis of bulk materials, heat flow, fluid flow and magnetism.

This article describes how to use the Autodesk Inventor Professional iLogic tool to design self-propelled drilling rigs. The parameterized, automatic generator of self-propelled drilling rigs allows for quick creation and modification of the conceptual model. It enables the verification of the machine's mobility and a preliminary assessment of its stability. Face Master 2.8 ATEX drilling rig by Mine Master, was the object of the described research work.

The use of advanced design methods is the subject of research work by various authors. There is an article about computer simulations and virtual reality applied in redesigning process of underground transportation routes [3]. The next ones are related to CAD systems in testing the collision of underground transportation means [4] and a train wagon in a narrow tunnel [5]. Another one is about using computer-aided design in Virtual Reality versus traditional 3D designing [6].

There are articles presenting the application of various IT tools used in the design of machines for ore mining [7-9]. The next ones concern the design of shearer loader's cutter head with the use of iLogic [10-11]. In the following article, the authors presented the use of modelling to develop a concept of a unique machine for securing the roofs of roadways with roof support [12].

The theoretical model for assessing the stability of self-propelled drilling rigs with single and double booms is known from the literature [13]. The cited article presents all the formulas and discusses the spreadsheet that allows for the evaluation of the stability of the drilling rigs. Moreover, the results of empirical research work confirming the correct operation of the spreadsheet are presented.

The article presents the use of CAD software, namely the iLogic tool of the Autodesk Inventor program, for the design of drilling rigs. The use of the iLogic tool allows for a quick assessment of working area and turning circle with simultaneous, continuous control of the position of the center of gravity.

2. Materials and Methods

2.1. Parametric 3D model of the drilling rig

Self-propelled mining machines, such as wheel-tyre drilling rigs, are of an articulated structure which, due to the use of booms, working conditions and requirements for turning circle, is prone to loss of stability. Drilling rigs are designed for specific user requirements that depend on the target workplace. The development of parametric iLogic models in Autodesk Inventor Professional allows you to quickly modify the geometry of the machine and verify the movement capabilities, the working area, while controlling the location of the center of gravity of the machine. The use of such a tool



speeds up conceptual work and allows for a relatively short time to specify the dimensions of each component of the machine, thanks to which it meets the user's requirements and is stable at the same time.

A parametric model was developed in the Autodesk Inventor Professional environment on the basis of the initial structure of the Face Master 2.8 ATEX twin-boom drilling rig by Mine Master. The machine combines parameterized subassemblies made with classical modelling and with the use of iPart parts (hydraulic cylinders). Everything is primarily controlled by the iLogic tool. In addition to the machine model, the selected components of the working creating the area simulating the face and the face-end were developed. The developed models were simplified as much as possible to enable quick change of parameters of the machine, without overloading the workstation. However, they still allow for a precise analysis of both the work area and the ability to pass face-end. The tool developed in this way allows to analyse the relationships among all machine parameters as well as the turning parameters and the position of the working parts on the work area and turning circle. During these analyses, the model enables continuous tracking of the location of the machine's gravity centre, including taking into account the workings inclinations. The FM 2.8 ATEX machine is divided into a drivetrain, a platform and working parts consisting of a boom and a guide frame with actuators, turntables and connectors. The machine as a parametric 3D model is shown in Fig. 1.

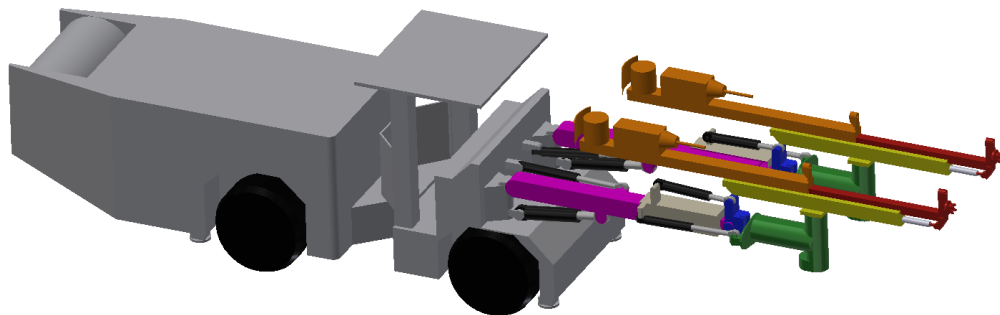


Fig. 1. View of the parametric model of FM 2.8 ATEX rig

All these components were parameterized taking into account also the mass and the coordinates of the gravity center of these components. The following figures show the parameters adopted for the drivetrain (Fig. 2), platform (Fig. 3) and the working part (Fig. 4). The gravity centres are marked with red dots.

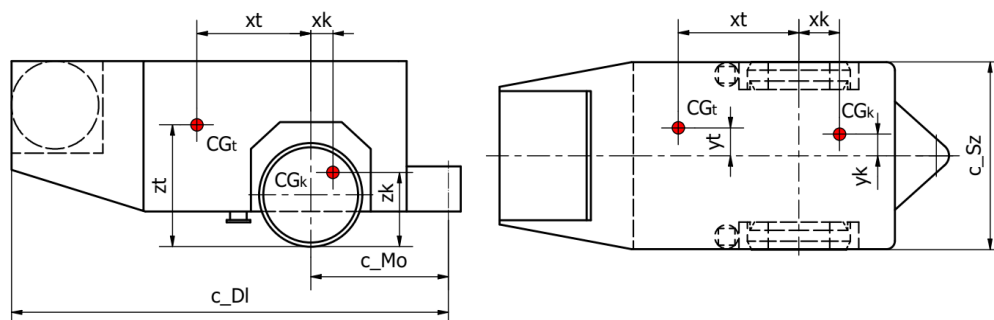


Fig. 2. FM 2.8 ATEX drivetrain with parameters

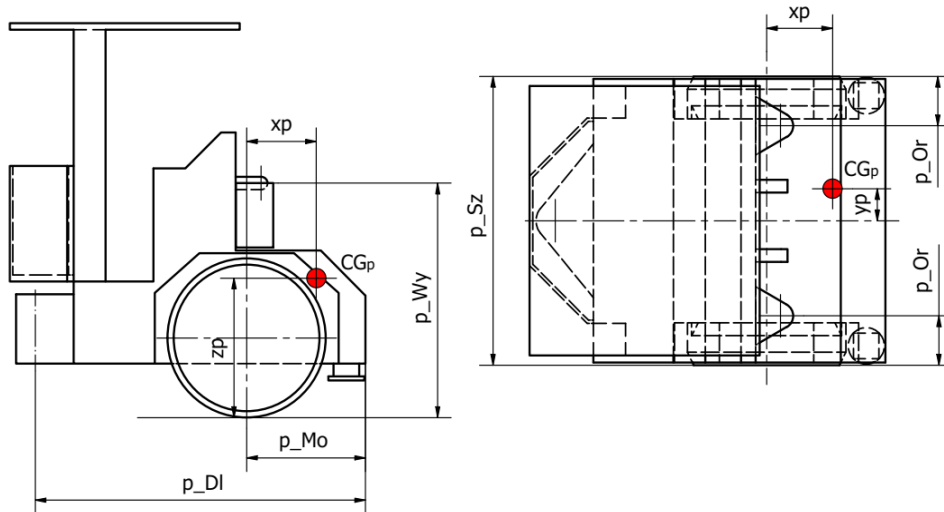


Fig. 3. FM 2.8 ATEX platform with parameters

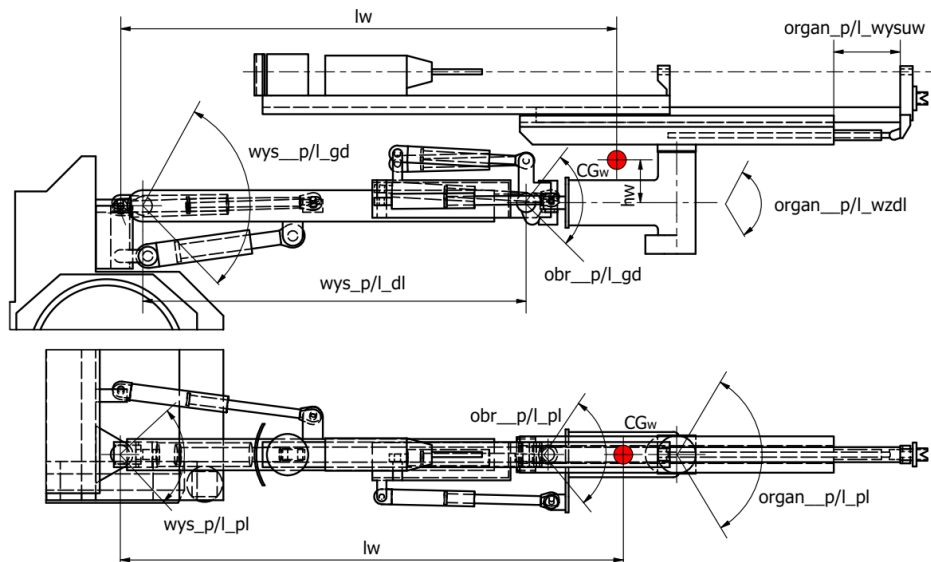


Fig. 4. FM 2.8 ATEX working part with parameters (original language of the schemes and forms)

The 3D model of subassemblies is fully parameterized and its geometry depends only on the provided dimensions. The rest of the geometry is related to the proper relationships. The masses, on the other hand, were modelled with spheres of constant density and diameters resulting from the mass of each component. Scripts convert the size of the spheres, so that the total weight and the position of gravity centre of the machine correspond to reality (Fig. 5).

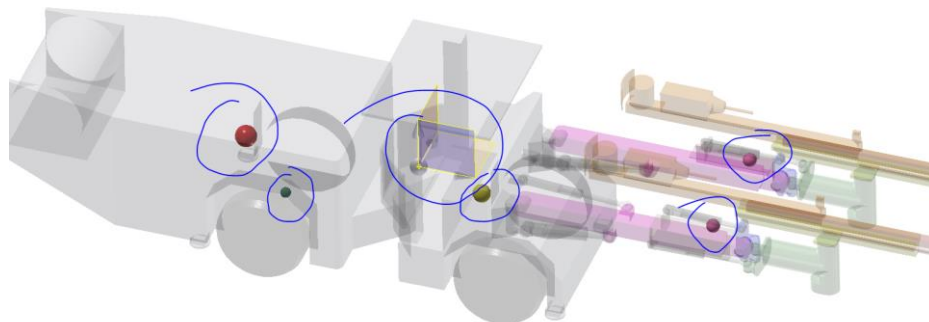


Fig. 5. Model 3D FM 2,8 ATEX with masses and the gravity centre

2.2. Parametric 3D model of the working

Apart from the machine, the parameterized face (Fig. 6) and the face end with turning circle (Fig. 7) were modelled. In the case of a face, the machine is at a level marked as "floor under the machine" and from this position it can make the entire contour creating a new floor below the level marked as "floor made by the machine"

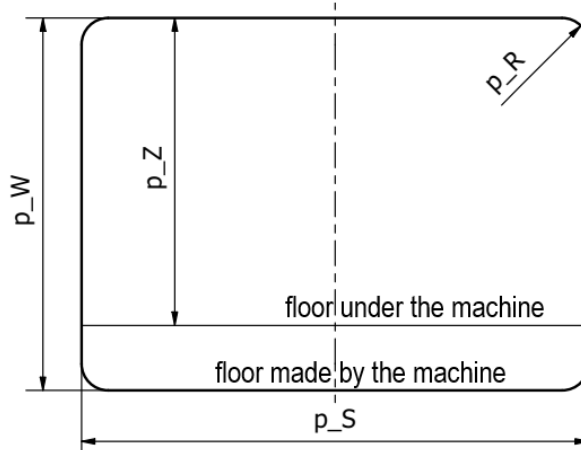


Fig. 6. Face cross-section with the parameters

In the case of a face end, two perpendicular roads with the width s_{Sz} were marked. Regardless of that, the inner radius s_{Rw} and the outer radius s_{Rz} are plotted. Taking into account the possibility of cutting the corner of the working by s_{Sc} , we obtain the withdrawal of the internal arc by the value marked as "gain", which results in the possibility of reducing the external turning circle.

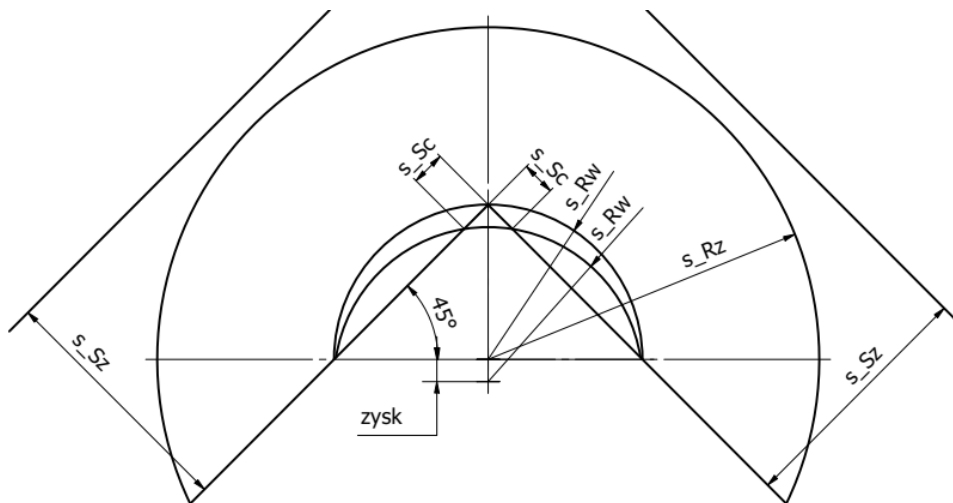


Fig. 7. Top view of a face end with marked turning radii and parameters

The location of the centre of gravity of the machine is independent of the pit inclination. From the stability point of view, only the vertical projection of the centre of gravity on the ground can be considered. The coordinates of the projections depend on the z_c coordinate of the centre of gravity and the longitudinal (α) and transverse (β) inclination. Knowing the coordinates of the centre of gravity and the inclination of the working, the following can be written:

$$x_{cn} := x_c - z_c \cdot \tan(\alpha) \tag{1}$$

$$y_{cn} := y_c + z_c \cdot \tan(\beta) \tag{2}$$

In the 3D environment a graphical method based on the given relationships can be used. The graphical method allows to determine the impact of the inclination on the stability of the machine by analysing the distance of the centre of gravity from the tipping edge, without calculations. Fig. 8 shows a machine with a prism of a triangle base defined by the tipping edges of the machine.

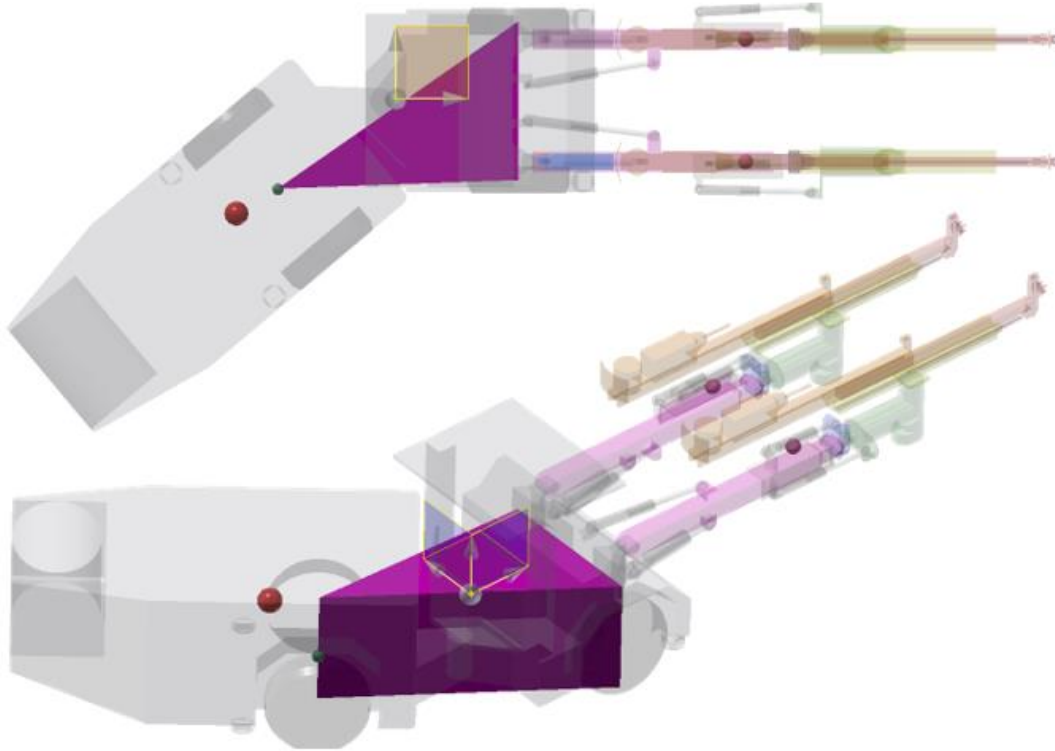


Fig. 8. A prism defining the stability in a horizontal working – machine in a turning position

Regardless of whether the working is inclined or not, the lower base of this prism is marked by the same three points delineating the triangle of the tipping edges (Fig. 9). On the other hand, its upper base runs at the height of the centre of gravity of the machine and is determined by three points shifted by the values described earlier, and resulting from the working inclination angles. So in an inclined working, the centre of gravity remains unchanged and the stability triangle moves. By analysing such a model in a plan view from above, you can easily determine the distances from the edge of the tipping in a horizontal and inclined working.

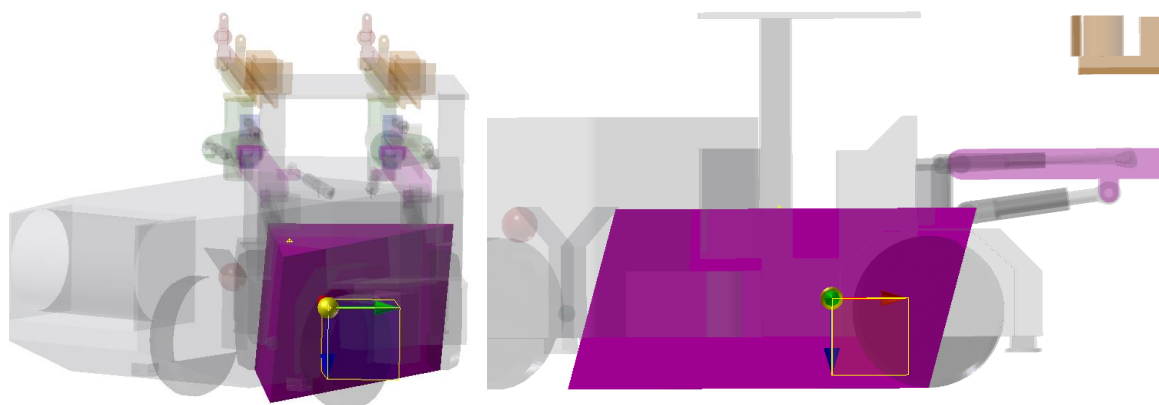


Fig. 9. Modification of the prism in an inclined working

2.3. Modification of the model using the iLogic

Using the parameters of the machine models required the creation of appropriate scripts and forms. Such possibilities are given by the iLogic tool. The scripts realize the simple commands and operations such as mass updating, arithmetic calculations, changing the machine geometry, controlling the turning of the machine and booms. Generally, the scripts allow determining the necessary relationships, calculate the indispensable quantities and superior control of the entire assembly. Forms are a tool that allows the user to enter each value. Four forms were created to operate the machine: "Chassis Geometry" and "Booms Kinematics" (Fig. 10), and "Global Settings" (Fig. 11) and "Stability" (Fig. 12). Geometry of the chassis allows setting the dimensions of the drivetrain and the platform, while the kinematics of the booms on two tabs determining the angles of rotation and extension of the left and right working component. The Global Settings form allows turning on or off the face and face end view, restore the machine geometry and kinematics to default values, turn on the left head copy position, straight line function, and including the tangency for inside turn radius analysis. In addition, the global settings form has two tabs that enable setting the turning parameters of the machine and the dimensions of the face and face end depending on the previous analysis.

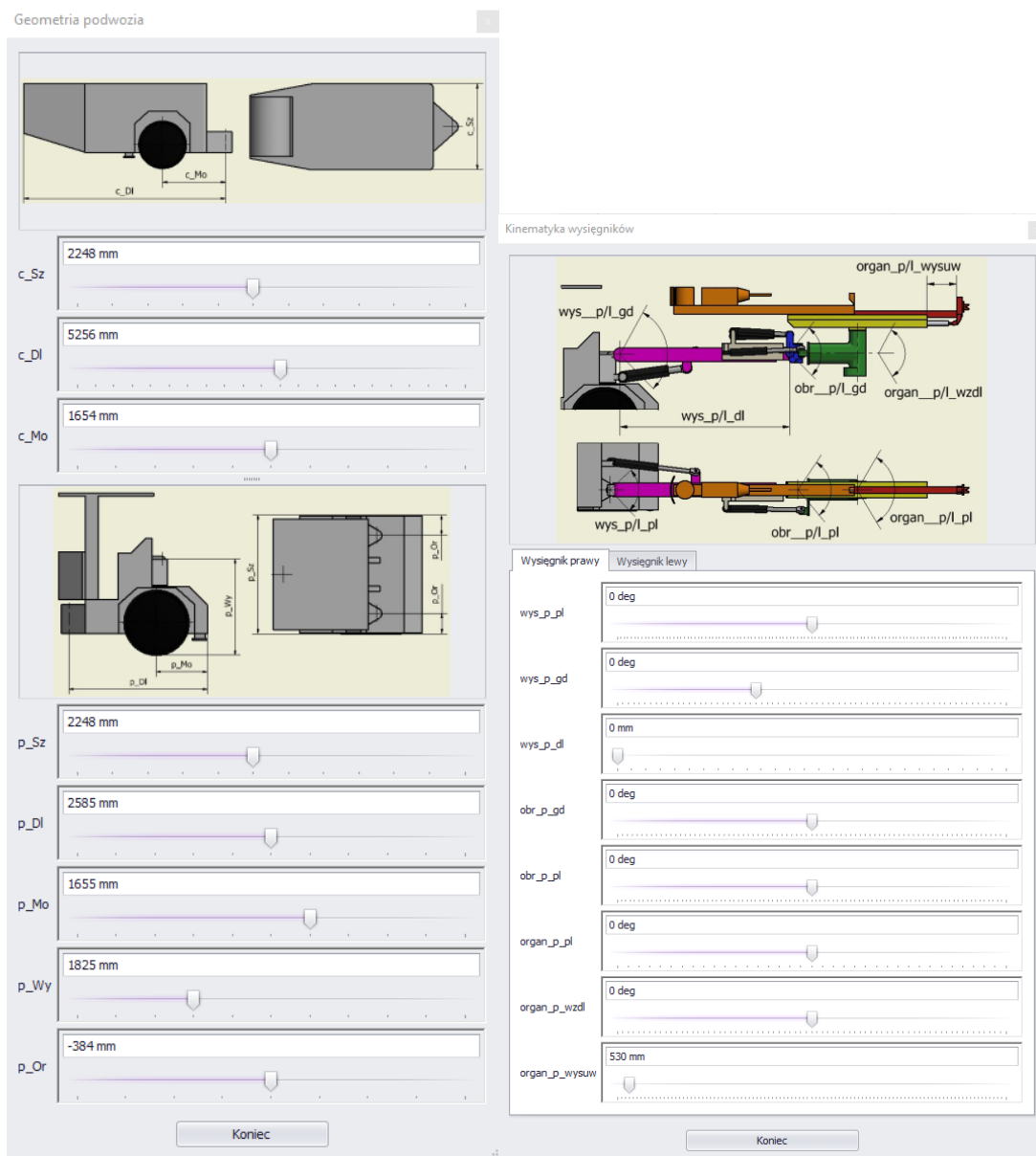


Fig. 10. The forms: chassis geometry and booms kinematics (original language of the forms)



The Stability form allows determination of the coordinates of the location of all centres of gravity and the mass of each component. In addition, it is possible to set the longitudinal and transverse inclination angles of the working. After selecting the boom extended or retracted option, the stability form needs to be updated with the "Update booms" button ("Update wysięgniki" in Polish shown in Fig. 12, on the left side). Any change in this form that affects the position of the centre of gravity must be updated with the "Update GC" button shown in Fig. 12 (the right form). After updating, the current coordinates of the machine's gravity centre can be read. The model is related to a 2D drawing with a top view, in which the distances of the centre of gravity from the tipping edges are constantly updated for the horizontal and inclined workings.

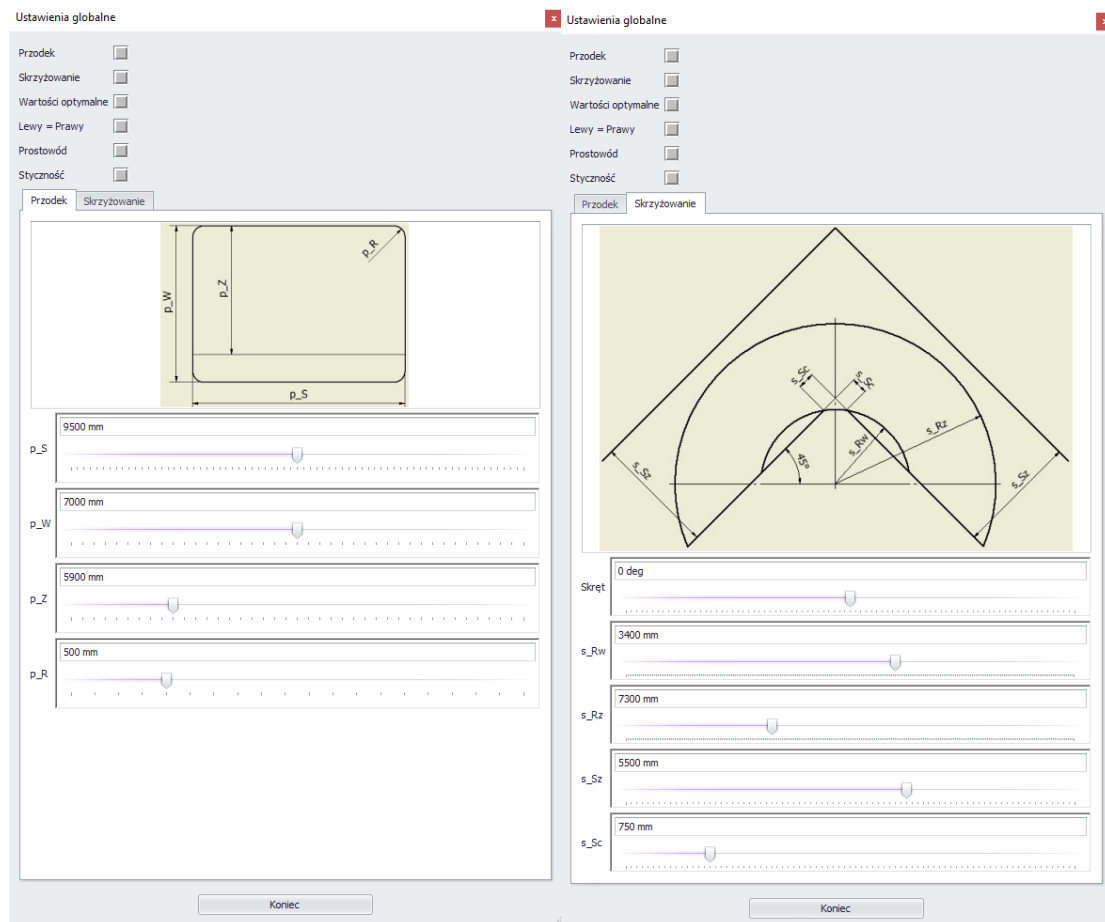


Fig. 11. Form of global settings: face, face end (original language of the forms)

Staceczność

Ciągnik

CGt 14363 kg

xt 575 mm

yt 90 mm

zt 1347 mm

Platforma

CGp 8060 kg

xp -540,5 mm

yp -65 mm

zp 1309,31 mm

Wysięgnik

CGw 3515 kg

lw_wys wsunięty_min wysunięty_max

Update wysięgniki

Kołyśka

CGk 1687 kg

xk 0 mm

yk -10 mm

zk 619 mm

opóźnienie 0 m/s²

nach_alfa 0 deg

nach_beta 0 deg

Update GC

CGx 207,160561978062

CGy 24,1457931920425

CGz 1468,20283558123

Koniec

Fig. 12. Stability form (original language of the forms)

2.4. Model tests of work area and a turning circle

The developed parametric model allows generating the unlimited number of configurations of each parameter. For each configuration, the working area and turning circle can be verified. During the model tests of the FM 2.8 ATEX machine, a set of parameters developed during the preliminary tests was used, which are presented in Table 1 and in Fig. 13.

Table 1. Maximum turning circles as well as telescope articulation and extension for FM 2.8 ATEX

Machine kinematics		
Parameter	Symbol	Range
Machine turning angle	γ	-40° ÷ +40° -42° ÷ +42°
Booms articulation - vertical	α_w	-25° ÷ +45°
Booms articulation - horizontal	β_w	-35° ÷ +35° -55° ÷ +55° - for $\alpha_w = \text{max}$
Extension of the telescope boom	Δw	0 mm ÷ 1350 mm

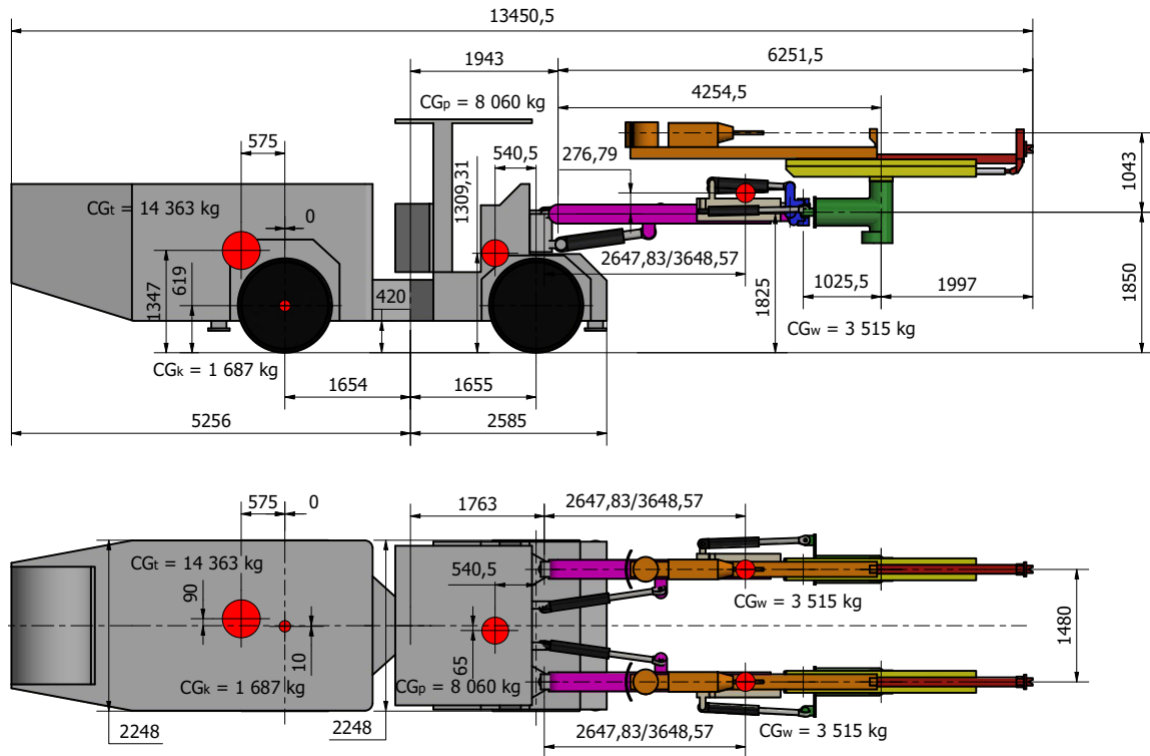


Fig. 13. Key dimensions of FM 2.8 ATEX assumed in iLogic

The machine model, according to the previously mentioned parameters, was simulated to verify the possibility of achieving the assumed working area and turning circle. This is one of the possibilities of using the parametric iLogic model, which is used at the end of the conceptual work. At the earlier stages, it is possible to search for the working area and turning circle for specific machine parameters or vice versa. Fig. 14 shows the selected views from the working area analysis, and Fig. 15 shows the turning circle analyses.

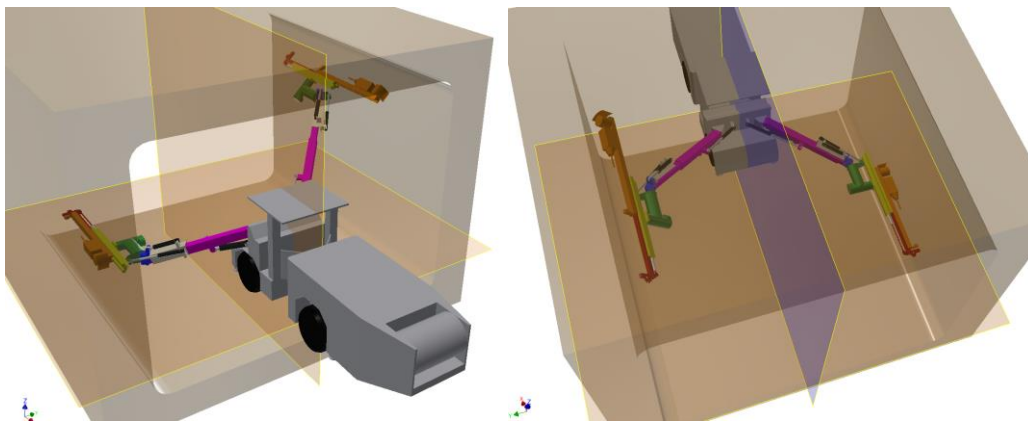


Fig. 14. Selected views of one of the working area FM 2.8 ATEX analyses

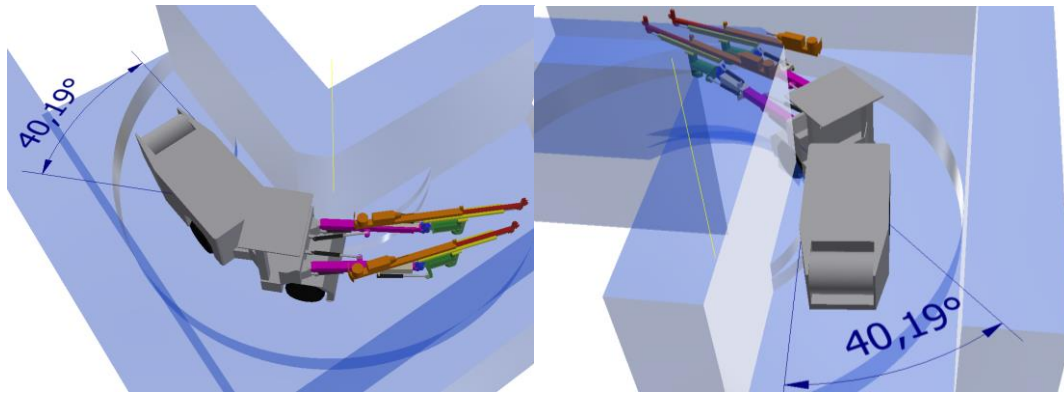


Fig. 15. Selected views of one of the vehicle passing the face end FM 2.8 ATEX analyses

Analysis of the work area confirmed the possibility of obtaining the work area assumed by the user, 9150 mm wide and 7000 mm high, of which 5900 mm at the height from the floor (Fig. 16). Areas of this size are obtained by deflecting the booms to the extreme positions and by extending the booms by 1350 mm.

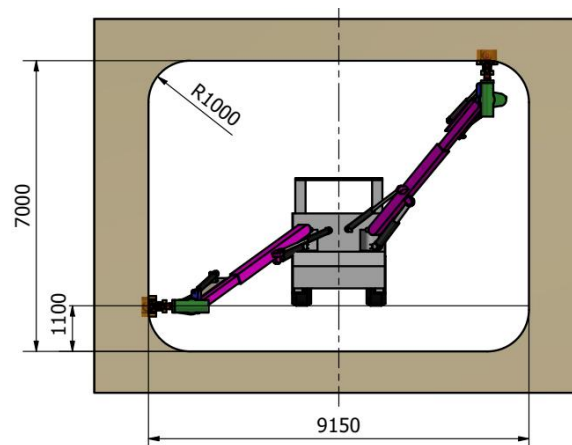


Fig. 16. Analysis of work area for FM 2.8 ATEX – full area – front view

Initially developed chassis and working components covering the assumed work area were used for further analyses of passing the workings. For FM 2.8 ATEX, several dozen analyses of passing the perpendicular workings were performed. Various positions of the car and the working components were simulated to obtain the assumed and required by the future user the turning circle of 3400 mm inside and 7300 mm outside. A series of analyses were performed to obtain the outer radius of 7300 mm. The assumed effect was achieved for the booms articulated by 10° and 5° and guide frames turned by 15° and 20° (Fig. 17).

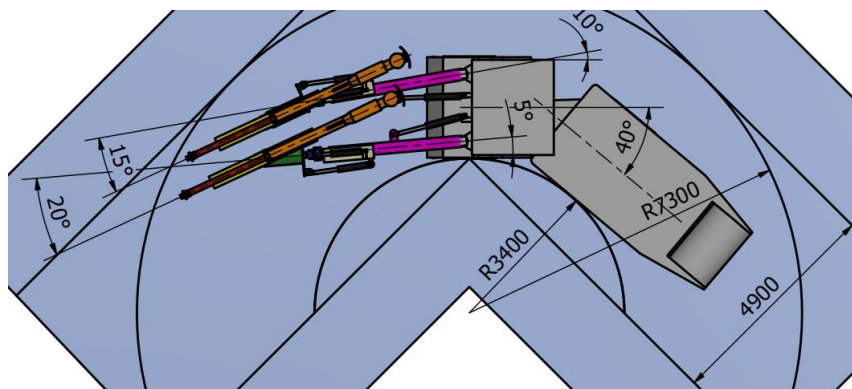


Fig. 17. Analysis FM 2.8 ATEX – booms articulated by 10° and 5° , frames turned by 15° and 20°

Assuming the possibility of cutting the working corner, its size can be selected so that the machine can pass the assumed excavation without manoeuvring the working parts. A corner rounding allowing the straight pass with the booms (Fig. 18) in a results in gaining 1400 mm. This is a borderline situation, i.e. for a 3400 mm cut, the machine can pass with the booms straight ahead. However, the cutting area is large and amounts to 2.47 m². By a slight articulation of the booms, the required area of cutting can be significantly reduced.

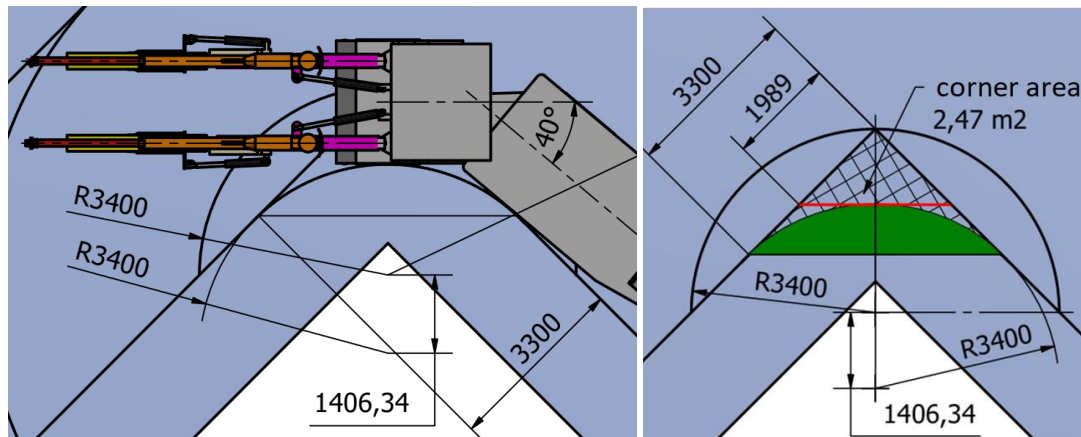


Fig. 18. FM 2.8 ATEX analysis – cutting the corner enable passing the machine with the booms straight ahead

3. Results – machine stability control

During the model tests, position of the machine's gravity centre against the background of tipping edges was verified. Each scenario, during the machine is turning or with the booms articulated was analysed. Sample results of the analysis of the distance of the gravity centre from the tipping edges during assessing the turning circle are shown in Fig. 19.

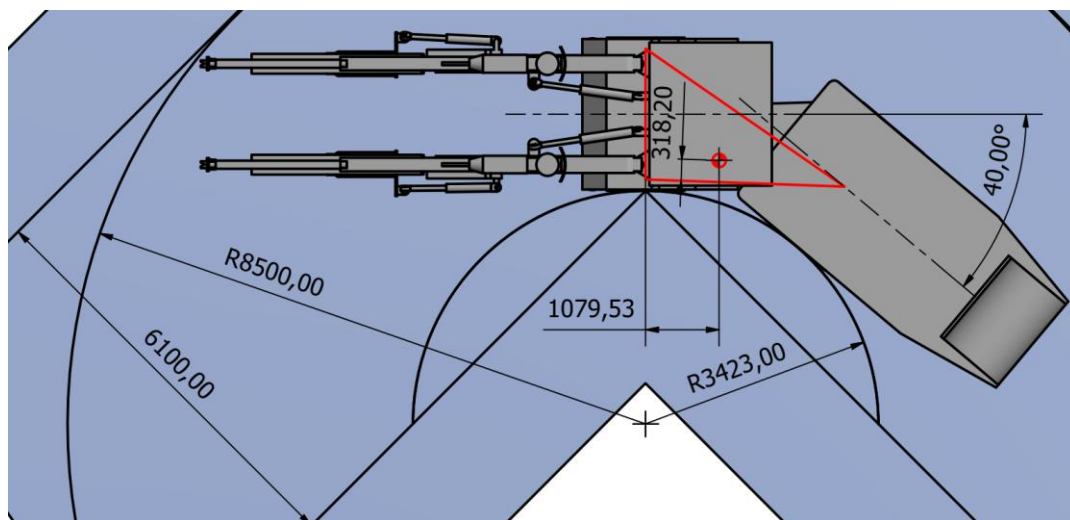


Fig. 19. FM 2.8 ATEX – R_w 3423 mm, R_z 8 500, S_z 6 100 mm, analysis of turn

Using the previously described graphical method, the impact of workings inclination on the stability, the distance of the gravity center from the modified tipping edges was determined. Sample analysis for a -15° longitudinal inclination and a 6° transverse inclination was shown in Fig. 20. The gravity center of the machine remains the same, but the tipping edges shift. The analysis was carried out simultaneously for two stability triangles, the red one defines the tipping edges for the horizontal working, and the green one for the inclined one. As a result, the figure shows the impact of specific workings inclinations on the change in stability of the machine.

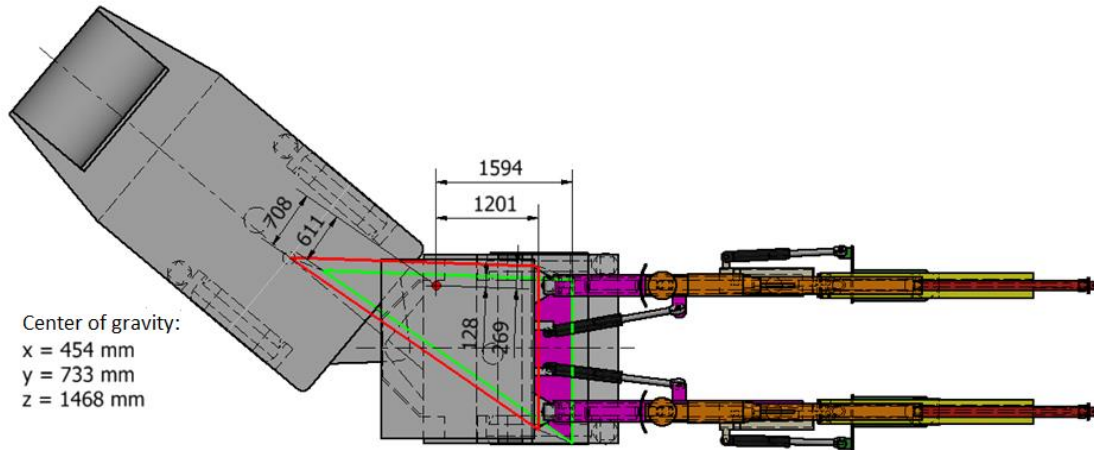


Fig. 20. A sample analysis of graphical interpretation of the impact of workings inclination

4. Conclusions

Confirmation of the parametric iLogic model correct operation was the key element in the work on its creation. At the stage of verification of the iLogic model, all results were checked against the theoretical model saved as a spreadsheet. Due to the different nature of both tools, the global coordinates of the rear wheels and rocker as well as the gravity centre of the drivetrain, rocker and booms were checked and compared. The rear end of the machine only turns, so the verification was limited only to changing one angle. The booms, on the other hand, are the complex mechanism where the position of their centre of gravity is affected by two boom angles and min/max extension. Fig. 21 shows an exemplary comparison of the results from the theoretical model and iLogic for the same variables. The results are identical.

Właściwości ogólne

Masa: 3515,000 kg (Błąd)

Pole: 111798,080 mm²

Objętość: 3515000,000 mm³

Środek ciężkości

X: 3260,885 mm (Błąd)

Y: -2879,202 mm (Błąd)

Z: 740,792 mm (Błąd)

Właściwości bezwładnościowe

Główne | Globalne | Środek ciężkości

Momenty główne

I1: 12508631,563 | I2: 12508631,563 | I3: 12508631,563

Obrót względem głównych

Rx: 0,00 deg (Błąd) | Ry: 0,00 deg (Błąd) | Rz: 0,00 deg (Błąd)

Data to be verified CG _{wp} :		
α_{wp}	β_{wp}	I_w
-30.0 deg	55.0 deg	2 647.8 mm

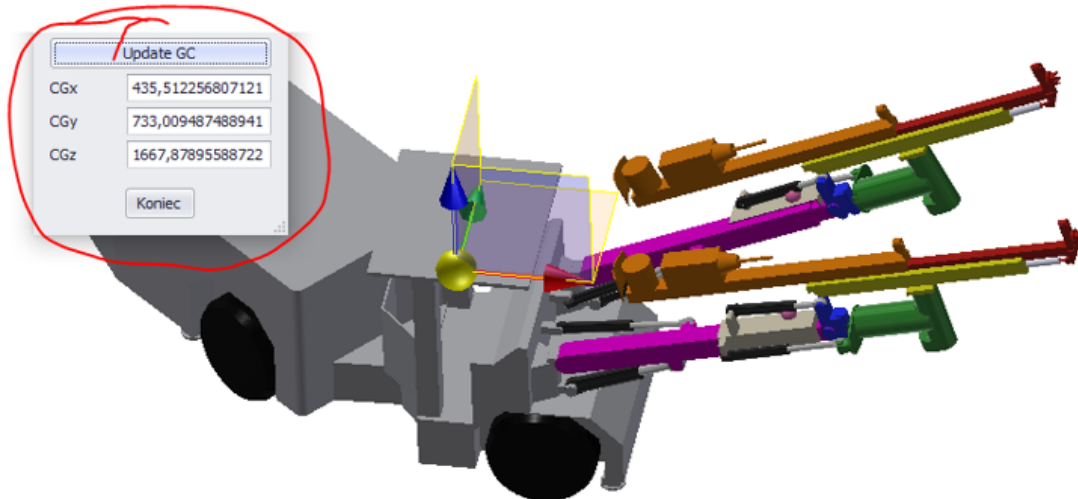
Boom centre of gravity:		
x	y	z
3 260.89 mm	-2 879.20 mm	740.79 mm

Fig. 21. Exemplary comparison of global coordinates of the iLogic model and the theoretical model – boom extended (original language of the properties window)

Similarly, the coordinates of the machine were compared for several selected situations, while different turning and deflection angles of the booms as well as the min/max extensions of the working parts from the straight-ahead position, but with the max extension of the working parts were checked. Comparison is shown in Fig. 22. During the verification, the turning circle and the distance of the gravity centre from the tipping edge were also checked. The results were identical.

The use of parametric modelling speeds up the design work, especially at the stage of concept development or preliminary design. Self-propelled drill rigs are the complex machines. Almost every

change in their geometry affects the working area, turning circles and changes the position of the machine’s centre of gravity. The issue of stability of the machines, especially articulated machines, is a serious problem that requires an appropriate approach from the very beginning of the designing process. In the case of drilling rigs, we are dealing not only with an articulated structure of the body, but also with long booms extending significantly beyond the undercarriage. Due to the way of manoeuvring in the workings and the arrangement of the booms, the machine moves or works on the verge of stability. Thanks to the developed parametric model, it is possible to modify the geometry of the machine in order to obtain the possibilities assumed and required by the user, while simultaneously controlling the position of its of gravity centre against the background of the tipping edge, both for horizontal and inclined workings. The forms are clear and easy to use, which significantly speeds up the creation of subsequent combinations of parameters.



Data for verification of the machine centre of gravity:					
γ	α_{wl}	β_{wl}	α_{wp}	β_{wp}	l_w
-40.0 deg	25.0 deg	0.0 deg	15.0 deg	0.0 deg	2 647.8 mm

Machine centre of gravity:		
x	y	z
435.51 mm	733.01 mm	1 667.88 mm

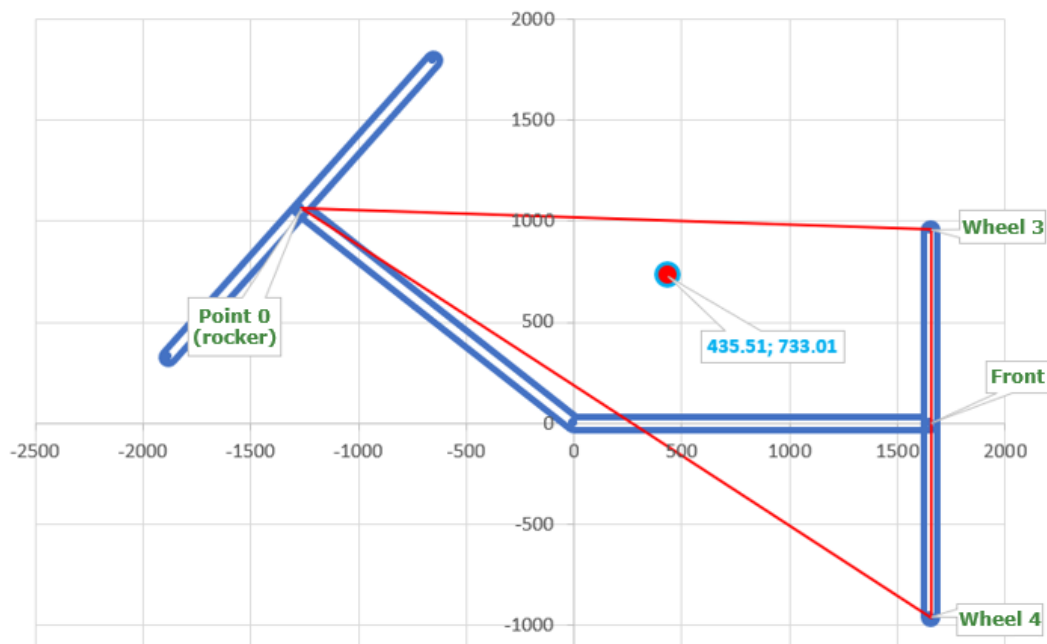


Fig. 22. Exemplary comparison of the center of gravity in the iLogic model and in the theoretical model

Funding:

The work was a part of the financial project of the National Centre for Research and Development "A modern set of multi-purpose self-propelled mining machines with computer-aided work of the operator, intended for development and protecting the roadways in underground mines and tunnels construction", POIR.01.01.01-00-0093 / 19-00.

References

- [1] Wang S.H., Melendez S., Tsai C.S., Wu C.W.: Parametric Design and Design Associability in 3D CAD. *Advanced Manufacture: Focusing on New and Emerging Technologies*. Vol. 594, 2008, pp. 461-468, DOI: 10.4028/www.scientific.net/MSF.594.461
- [2] Zhang ASJ.: Teaching computer aided product design with aesthetic considerations. *Proceedings of the ASME International Design Engineering Technical Conferences and Computers and Information in Engineering Conference 2005*, vol. 3, 2005, s. 581-584
- [3] Rozmus M., Tokarczyk J., Michalak D., Dudek M., Szewerda K., Rotkegel M., Lamot A., Roser J.: Application of 3D Scanning, computer simulations and virtual reality in the redesigning process of selected areas of underground transportation routes in coal mining industry. *Energies* 2021, nr 14(9) 2589, s. 1-21
- [4] Dudek, M.: Use of CAD Systems in Testing the Collision of Underground Transportation Means. *Arch. Min. Sci.* 2013, 58, s. 411–432
- [5] Schauer, J.; Nüchter, A. Collision detection between point clouds using an efficient k-d tree implementation. *Adv. Eng. Inform.* 2015, 29, 440–458
- [6] Feeman S.M., Wright L.B., Salmon J.: Exploration and evaluation of CAD modeling in virtual reality. *Comput. Aided Des. Appl.* 2018, 15, 892–904.
- [7] Bołoz Ł.: Digital prototyping on the example of selected self-propelled mining machines. *Multidisciplinary aspects of production engineering: monograph. Pt. 1, Engineering and technology*, ed. Jacek Sitko, Warszawa, Sciendo, 2020
- [8] Bołoz Ł., Ostapow L.: Prototypowanie cyfrowe na przykładzie wybranych samojezdnych maszyn górniczych. *Transport Przemysłowy i Maszyny Robocze: przenośniki, dźwignice, pojazdy, maszyny robocze, napędy i sterowanie, urządzenia pomocnicze*, nr 4, 2020, s. 59–66
- [9] Vališ D., Gajewski J., Forbelská M., Vintr Z., Jonak J.: Drilling head knives degradation modelling based on stochastic diffusion processes backed up by state space models. *Mech. Syst. Signal Process.*, 2022, Vol. 166, 108448, <https://doi.org/10.1016/j.ymsp.2021.108448>
- [10] Bołoz Ł.: Generowanie parametrycznych modeli organów frezujących kombajnów ścianowych. *Modelowanie Inżynierskie, Wydział Mechaniczny Technologiczny Politechniki Śląskiej*, t. 40 nr 71, s. 13–18, 2019
- [11] Bołoz Ł., Castañeda L. F.: Computer-aided support for the rapid creation of parametric models of milling units for longwall shearers, *Management Systems in Production Engineering*, vol. 26, iss. 4, 2018, pp. 193–199, DOI: 10.1515/mspe-2018-0031
- [12] Bołoz Ł., Mendyka P.: Koncepcje wozów samojezdnych do zabezpieczania stropów wyrobisk korytarzowych obudową powierzchniową. *Transport Przemysłowy i Maszyny Robocze: przenośniki, dźwignice, pojazdy, maszyny robocze, napędy i sterowanie, urządzenia pomocnicze*, nr 2, 2018, s. 42–46
- [13] Bołoz Ł., Kozłowski A.: Methodology for assessing the stability of drilling rigs based on analytical tests. *Energies*, 14, 24, 8588, 2021, pp. 1-29, <https://doi.org/10.3390/en14248588>



<https://doi.org/10.32056/KOMAG2022.3.6>

Shaft reaming machine for maintenance of mine shafts in the salt rock mass

Received: 12.09.2022

Accepted: 27.09.2022

Published online: 11.10.2022

Author's affiliations and addresses:

¹ KOMAG Institute of Mining Technology, Pszczyńska 37, 44-101 Gliwice, Poland

² Coal Mine Velenje, d.o.o., Partizanska cesta 78, 3320 Velenje, Slovenia

* Correspondence:

e-mail: pkaminski@komag.eu

Paweł KAMIŃSKI ^{1*}, Darian BOŽIČ²

Abstract:

Due to rheological properties of salt rock mass, maintenance of mine excavations, including shafts may be very challenging, especially in the long term. Many different ideas and approaches to a subject of sinking and maintaining a shaft in salt rock mass have emerged over the years, of which the main directions include two opposite ideas, such as an application of high-strength lining and an approach based on flexible lining. The article presents a shaft reaming machine designed for maintenance of mine shafts located in salt rock mass designed with a flexible shaft lining approach.

Keywords: mine shaft, shaft maintenance, salt rock mass, salt mining, mine safety, shaft reaming machine



1. Introduction

In standard strength tests, rock salt shows rheological characteristics, reflected in creeping and stress relaxation. Creep process can be divided into three stages (as shown in Fig. 1):

- primary,
- secondary,
- tertiary.

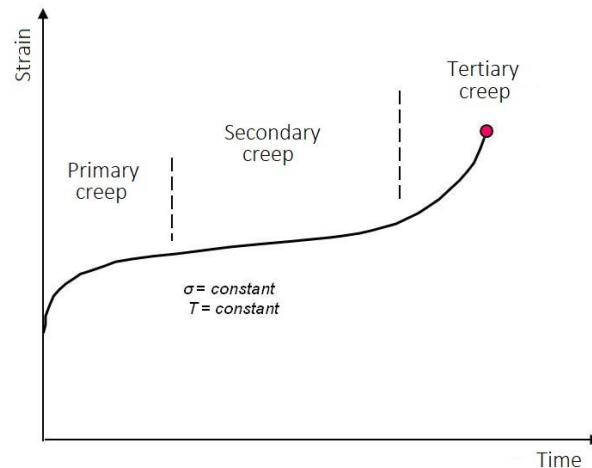


Fig. 1. Creep curve

Primary creep stage starts with a rapid rate – significant deformations occur within a short term. In the creep strain vs time graph it is projected as a steep curve. The material is subject to constant pressure, strain increase, but their rates decrease. This process lasts until the secondary stage begins, in which the creep rate is relatively uniform. Experiments show that the strain is dependent mainly on the stress conditions in the primary creep stage.

The creep process and thus the creep curve in the primary and secondary stages is dependent on two mechanisms: strengthening and regeneration. If those processes are in imbalance, the primary creep stage occurs, while in the case of their balance the equilibrium takes place. Creep rates decrease as the strengthening predominates over regeneration.

In the tertiary creep, the creep rate accelerates rapidly. The strain increases until the moment of material break or rupture. Volume of the rock sample increases in this stage due to an occurrence of microfractures, which are the main reason of the sample destruction [2-10].

Convergence is one of the key factors of stability and safety of mine shafts located in salt layers, as the sidewalls convergence is a source of major stress acting on the shaft lining. Thus the converge rate is a determinant of actions which should be undertaken to counteract its destructive impact on the shaft lining.

Experiments and practical experience show that sidewalls deformations caused by convergence may occur in a relatively short term. Thus, different approaches to shaft lining design have been used to solve the problem of its stability under the influence of convergence in salt rock mass. The first idea was to apply a high-strength steel lining, capable of bearing extremely high loads [10]. In contrast, an application of highly reactive, flexible lining was proposed and implemented in practice, e.g. in the SW-4 shaft at Polkowice-Sieroszowice mine, a part of the KGHM SA [11]. According to some experts [12] an implementation of a flexible shaft lining, providing hydraulic support with use of a column of fully saturated brine between typical watertight shaft lining (e.g. tubing lining) and shaft sidewalls, is more efficient.

High flexible shaft lining, implemented in the SW-4 shaft of Polkowice-Sieroszowice mine utilizes the coating made of composite mesh and layers of sprayed-applied polyurethane as well as mineral

protective layer and auxiliary support, comprising bolted yielding arches. The task of the mineral coating is a protection of the shaft sidewalls against the impact of flowing humid air, while the auxiliary support is used to prevent the shaft against potential rock mass fracturing consequences. The design of the lining allows for a deformation of both shaft sidewalls and of the lining itself. To ensure a proper air flow in the SW-4 shaft (as the shaft is an upcast ventilation shaft) a reconstruction of the shaft lining is required within a designed time interval up to 12 years. Shaft lining reconstruction consists of several stages, including a disassembly of the worn out shaft lining, reaming of the shaft sidewalls to the designed diameter and a installation of the new shaft lining.

In recent years, an idea of the shaft lining utilizing a characteristic feature of rock salt, which is water solubility appeared. This feature is generally considered a drawback in terms of mine workings' maintenance, however it may be used to control the load acting on the shaft lining. The key elements of the shaft lining design include preliminary shaft sidewalls bolting, tubing lining of modified construction, porous material filling of the annulus between the shaft sidewalls and the tubing shaft lining and a system of pipelines, pumps and tanks for the leaching medium circulation [13-14].

The idea of the described shaft lining is based on periodic leaching of the shaft sidewalls in the controlled process carried out in the annulus between the tubing lining and the shaft sidewalls. Such design allows for simultaneous shaft lining "reconstruction" (leaching of the shaft sidewalls) and typical shaft operation, including airflow, men-riding, transport of materials and media to and from the mine workings. Experiments were carried out to verify assumptions and validate a possibility of implementing such a construction in a mine shaft. They allowed also for a determination of parameters of the designed shaft lining and leaching medium. The effects of the tests are optimistic, however real-life tests in mine shafts are indispensable to verify the results in practice [13-16].

2. Materials and Methods

Shaft reaming machine

The designed and patented shaft reaming machine may be applied for shaft liquidation and reconstruction operations. Its base is a working platform suspended on steel ropes. It consists of three sections:

- top section,
- reaming section,
- loading section.

The reaming section is separated from the other sections with two platforms – the top platform dividing it from the top section and the bottom platform separating it from the loading section. The device is equipped with a tubular guide for a conveyance (typically shaft bucket) which is located in the shaft axis and allows for men-riding and transporting material to and from the top and loading sections. The top and loading sections are also equipped with stabilizers which are used to support and stabilize the reaming machine at the level on which it is used. The reaming section is equipped with a frame, which is an angular truss construction to which a boom of a cutting head is attached. The truss construction and the tubular guide are connected with bearings.

The main goal of the presented machine designers was a design and a construction of a lightweight reaming machine, which allows for controlling the cutting head web depth, an easy stabilization of the device on the cutting level, suitable for intervention activities and facilitating loading and hauling processes [17-18]. A view of the shaft reaming machine is presented in Fig. 2.





Fig. 2. A view of the shaft reaming machine

The key structure of the reaming section is the frame to which both the cutting head boom and operator's cabin are assembled. A gear rack allows for a vertical movement of the cutting head, while the bearing connecting the truss construction with the top platform and the tubular guide is responsible for a rotational movement of the whole construction and thus of the cutting head [17].

The diameter of the bottom platform is smaller than the loading deck diameter, which allows for a gravitational transport of the excavated material to the loading deck, from where it is loaded into buckets and hauled to the surface. The stabilizers, attached to the bottom platform, allow for horizontal and vertical positioning of the machine, which in turn enables a greater adjustability of the cutting head web depth. The design of the cutting head boom and its attachment to the frame allows for controlling a vertical position of the cutting head position and of the cutting head web depth [17].

The design of the shaft reaming machine is presented in Fig. 3 and 4.

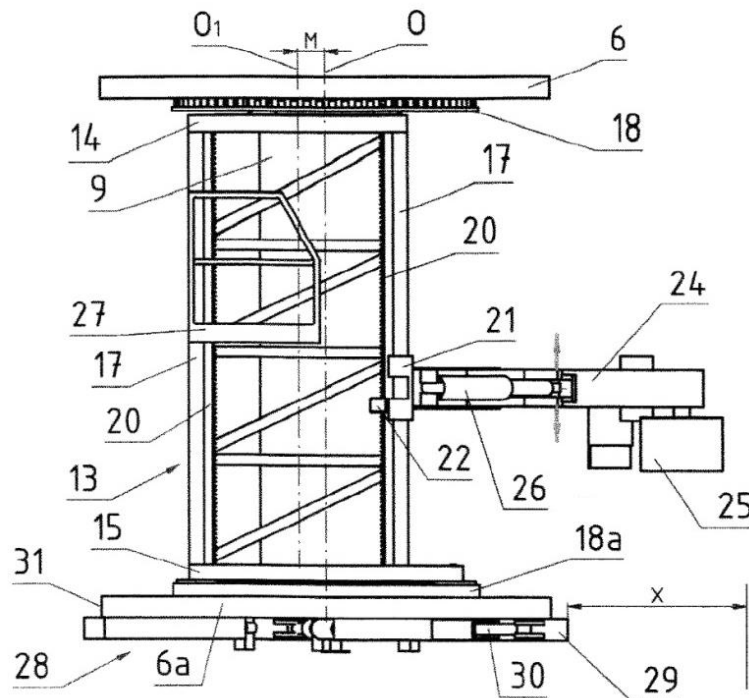


Fig 3. Vertical presentation of the shaft reaming machine [16]

6 – top platform, 6a – bottom platform, 9 – tubular guide, 13 – frame, 14 – top bearing, 15 – bottom bearing, 17 – truss, 18 – top ring, 18a – bottom ring, 20 – gear racks, 21 – horizontal adjustable beam, 22 – cutting head drive, 24 – cutting head boom, 25 – cutting head, 26 – hydraulic cylinder, 27 – operator's cabin, 28 – hydraulic stabilizer, 29 – stabilizer's beam, 30 – hydraulic cylinder, 31 – outline of the bottom platform;
M – eccentricity, O – horizontal axis of the shaft reamer, O₁ – axis of the frame

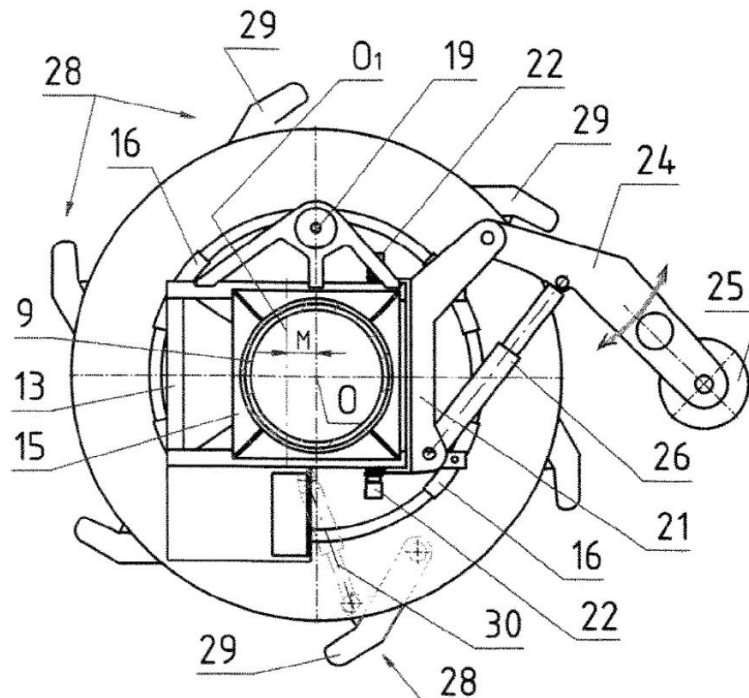


Fig. 4. Horizontal view of the shaft reaming machine [16]

9 – tubular guide, 13 – frame, 15 – bottom bearing, 16 – guidance, 19 – drive, 21 – horizontal adjustable beam, 22 – cutting head drive, 24 – cutting head boom, 25 – cutting head, 26 – hydraulic cylinder, 28 – hydraulic stabilizers, 29 – stabilizer's beam, 30 – hydraulic cylinder;
M – eccentricity, O – horizontal axis of the shaft reamer, O₁ – axis of the frame

A small number of salt mines in Poland and thus a small number of mine shafts sunk and maintained in salt rock mass do not make a development of such a machine a sort of priority. However, in numerous countries of the world, including Germany, not only new solutions for mine shaft lining are developed but also shaft reaming and shaft sinking machines. A machine of similar construction is currently in use in one of German salt mines, which shows that the approach of flexible shaft lining for salt mines gains popularity.

3. Conclusions

Salt mining, although still remains in the shadow of other branches of the mining industry, is a field of continuous development. Specific characteristics of rheological salt rock mass require an application of solutions not feasible in other places, which applies also to shaft sinking and design of shaft lining. Conventional solutions, successfully used in numerous mine shafts over the world are not always suitable for an application in salt rock mass. It fosters a development of alternative solutions, of which flexible shaft lining is currently gaining popularity. Modern solutions of shaft lining with use of periodic leaching of the shaft sidewalls are also considered promising.

However, the problem of shaft lining in the sections located in salt rock mass does not concern only salt mines. KGHM SA, the biggest producer of copper and silver in Poland, has broad experience in sinking and maintaining mine shafts in the sections located in salt rock mass, as some of the shafts of the Company's copper ore mines are partially located in the salt rock mass. This is where the most modern flexible shaft lining construction in Poland has been applied.

Different designs and constructions of flexible shaft lining, similar to the one applied in the SW-4 shaft of Polkowice-Sieroszowice mine, require a periodic reconstruction of the shaft lining, such as activity is connected with periodic shaft operation stoppages, which can have a negative impact on the whole mine efficiency.

The shaft reaming machine presented in the article, enables to facilitate the process of shaft reaming in a mine shaft section located in the salt rock mass and supported with flexible shaft lining, similar to the solution implemented in the SW-4 shaft. Despite the cost of development and construction of the machine, it can help reduce costs of shaft maintenance due to a reduction of the shaft downtime. An application of a similar device in the German mining industry allows to conclude that a development of the flexible shaft lining and of the shaft reaming machine is reasonable due to economic and technological reasons.

References

- [1] Jaeger J.C., Cook N.G.W., Zimmerman R.: *Fundamentals of Rock Mechanics*, John Wiley & Sons, Hoboken, NJ, USA 2009
- [2] Jeremic M.L.: *Rock mechanics in salt mining*, Brookfield A.A. Balkema, Rotterdam 1994
- [3] Hunsche U., Hampel A.: *Rock salt - the mechanical properties of the host rock material for a radioactive waste repository*, *Engineering Geology* vol. 52(3-4), 1999, s. 271-291
- [4] Jackson M.P.A., Hudec M.R.: *Salt tectonics principles and practice*, Cambridge University Press, Cambridge 2017
- [5] Lotze F.: *Steinsalz und Kalisalz*, Gebrüder Berntraeger, Berlin 1957
- [6] Schuppe F.: *Untersuchungen über rheologische Eigenschaften von Salzgestein*, 1966
- [7] Höfer K.H., Thoma K.: *Triaxial tests on salt rocks*, *International Journal of Rock Mechanics and Mining Sciences & Geomechanics Abstracts*, 1968 vol. 5(2), s. 195-196
- [8] Serata S.: *Application of continuum mechanics to design of deep Potash mines in Canada*, *International Journal of Rock Mechanics and Mining Sciences & Geomechanics*, 1968 vol. 5(4), s. 293-314
- [9] Ślizowski J.: *Badania własności reologicznych soli kamiennej przy projektowaniu komór magazynowych gazu ziemnego w górotworze solnym (Research on rheological properties of rock salt in the process of design of high underground gas tanks in salt rock mass)*, *Przegląd Górniczy*, 2001 vol. 5, s. 9-15



- [10] Klein J.: Stresses in sliding-shaft linings due to curvature, presentation ob 3rd International Conference on Shaft Design and Construction, 12–16.04.2012, London
- [11] Fabich S., Morawiec P., Soroko K., Szlązak M.: Problemy z utrzymaniem obudowy powłokowej w interwale soli kamiennej szybu SW-4 kopalni ZG „Polkowice-Sierszowice” (Problem of maintenance of the shaft lining of the SW-4 shaft of Polkowice-Sierszowice mine in the section located in the salt rock mass), *Przegląd Górniczy*, 2016 vol. 72(3), s. 65–74
- [12] Chudek M., Kleta H., Wojtusiak A., Chudek M.D.: Obudowa szybów w warunkach znacznych ciśnień deformacyjnych górotworu (Shaft lining in conditions of significant deformative rock mass pressure), *Górnictwo i Geoinżynieria*, 2009, vol. 33(3/1), s. 87–90
- [13] Kamiński, P., Czaja, P.: An innovative solution to counteract convergence of shaft lining in rock salt strata, *Archives of Mining Sciences*, 64(2), 2019 s. 429–445
- [14] Kamiński P.: A New Method of Regulation of Loads Acting on the Shaft Lining in Sections Located in the Salt Rock Mass, *Energies*. 2021; 14(1):42
- [15] Kamiński, P., Cyran, K.: Stanowisko do badań obciążenia obudowy szybu zlokalizowanego w warstwach solnych zalegających na dużych głębokościach (Research device for lining effort measurements located on the large depth in rock salt layers), *Przegląd Solny*, 2014, vol. 10, s. 75–84
- [16] Kamiński P., Ahmad M.: LabVIEW based software for verification of the new idea of lining for mine shafts located in salt rock mass, *Mining Machines*, 2021, vol. 39 issue 3, pp. 45-57
- [17] Olszewski J., Kamiński P., Dobisz W., Korczyński M.: Urządzenie do poszerzania wyłomu szybu (Shaft reaming machine), Polish patent PL417676, 2016
- [18] Mieszczak M., Kamiński P.: Urządzenie do poszerzania wyłomu szybu górniczego (Shaft reaming machine), in: *Innowacje w górnictwie, Przedsiębiorstwo budowy szybów SA 2011-20, Przedsiębiorstwo Budowy Szybów S.A., Tarnowskie Góry*, 2021

